Chapter 6
Data Series as a Source for Modelling

When a model is constructed from "first principles", its variables inherit the sense implied in those principles which can be general laws or derived equations, e.g., like Kirchhoff's laws in the theory of electric circuits. When an empirical model is constructed from a time realisation, it is a separate task to reveal relationships between model parameters and object characteristics. It is not always possible to measure all variables entering model equations either in principle or due to technical reasons. So, one has to deal with available data and, probably, perform additional data transformations before constructing a model.

In this chapter, we consider acquisition and processing of informative signals from an original with the purpose to get ideas about opportunities and specificity of its modelling, i.e. the stage "collection and analysis of time series data" and "a priori information" at the top of the scheme in Fig. 5.1.

6.1 Observable and Model Quantities

6.1.1 Observations and Measurements

To get information necessary for modelling, one *observes* an object based on prior ideas or models at hand (Sect. 1.1). As a result, one gets qualitative or quantitative data. Qualitative statements may arise from pure *contemplation*, while quantitative information is gathered via *measurements* and *counting*. Counting is used when a set of discrete elements is dealt with, e.g., if one tries to register a number of emitted particles, to determine a population size and so forth. Measurement is a comparison of a measured quantity with a similar quantity accepted as a unit of measurement. The latter is represented by standards of various levels. When speaking of "observation", "observable quantities" and "observation results", one means a measurement or counting process, measured or counted quantities and resulting quantitative data, respectively (Mudrov and Kushko, 1976). It is widely accepted to omit the word "quantities" and speak of "observables". We denote observables by the letter η resembling a question mark to stress a non-trivial question about their possible relationships with model variables.

Any real-world system possesses an infinite set of properties. However, to achieve goals of modelling, it is often sufficient to consider a finite subset: *model variables* $x_1, x_2, \ldots, x_D$ and *model parameters* $c_1, c_2, \ldots, c_P$. The number of observables and model variables, as well as their physical meaning, may differ. Thus, the number k of observables $\eta_1, \eta_2, \ldots, \eta_k$ is usually less than a model dimension D. Quite often, observables have a meaning different from variables entering model equations. Anyway, observables are somehow related to the model variables. Such a relationship is determined by experimental conditions, accessibility of an original, its shape and size, lack of necessary equipment, imperfection of measurement tools and many other objective and subjective factors. For instance, opportunities of electric measurements inside a biological cell are restricted due to the small size of the latter (Fig. 6.1a). An oscillating guitar string is big and easily accessible so that one can measure velocity and coordinate of each small segment of this mechanical resonator (Fig. 6.1b). In contrast to that, an access to inner volume of a closed resonator can be realised only via holes in its walls, i.e. after partial destruction of an object (Fig. 6.1c).

Relationships between observables and model variables may be rather obvious. Both sets of quantities may even coincide. However, a simple relationship is more often lacking. In general, this question requires a special analysis as in the following examples:

(i) Evolution of a biological population is often modelled with a map showing dependence of the population size at the next year x_{n+1} on its size at the current year x_n. If experimental data η are gathered by observers via direct counting, then *a model variable and an observable coincide*: $x = \eta$. However, if one observes only results of vital activity (traces on a land, dung, etc.) and tries to infer the population size from them indirectly, then one needs formulas for the recalculation or other techniques to reveal a *dependence between x and η*.

(ii) Physicists are well familiar with measurements of electromotive force (e.m.f.) E of a source with internal resistance r_i with the aid of a voltmeter (Fig. 6.2a, b). An object is a source of current, a model variable is e.m.f. ($x = E$) and an observable is a voltage U on the source clamps. To measure U, a voltmeter is connected to the source as shown in Fig. 6.2a. Resistance between the input clamps of a real-world voltmeter R_v (input resistance) cannot be infinite, therefore, after connection the loop gets closed and current I starts to flow. Then, the voltage on the source clamps reduces as compared with the case
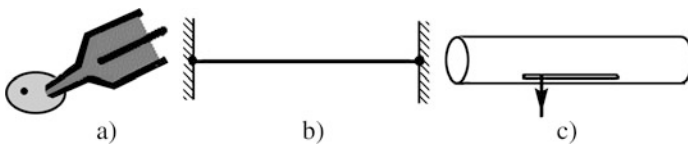

Fig. 6.1 Accessibility of different objects: (**a**) electric access to a cell via a glass capillary; (**b**) an open resonator; (**c**) a closed resonator
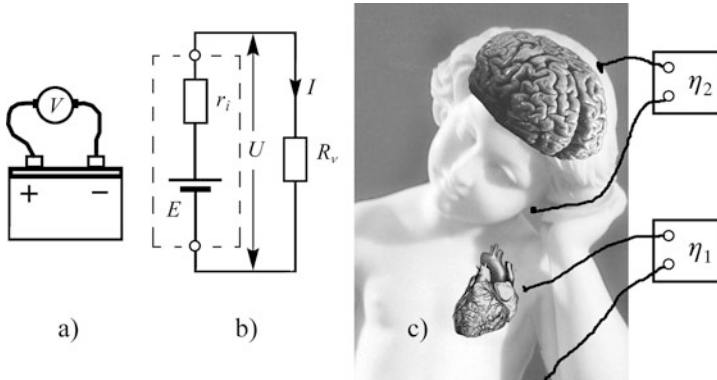
Fig. 6.2 Examples of characterising quantities and observables: (**a**) an experiment with a source of e.m.f.; (**b**) an equivalent scheme for the e.m.f. measurement; (**c**) observables in the analysis of brain and heart activity

without measurement device: $U = E - Ir_i = E\left(1 - r_i/(r_i + R_v)\right)$. Thus, the observable differs from the model variable, but *there is a unique functional dependence* between both quantities $\eta = f(x)$.

(iii) When electric potentials on a human skin are recorded, an observable η is a voltage between two points on a body surface. One of the points is taken as a reference (Fig. 6.2c). For an electroencephalogram (EEG) measurements, η is usually a voltage between points on a scalp and a ear; for electrocardiogram (ECG), it is a voltage between points on a chest and a leg. Even without special knowledge, one can see that the measured voltages are strongly transformed results of the processes occurring in ensembles of the brain cells or in the heart. Therefore, relationship between the observed potentials η and any model variables x characterising a human organism is a subject of special study. As mentioned in Sect. 1.6, a researcher is here in a position of passive observation of a complicated real-world process (Fig. 6.2c) rather than in a position of an active experimentation with a laboratory system (e.g. Fig. 6.2a). In particular, the greater difficulty of the passive case for modelling is manifested in a greater number of unclear questions. However, if a researcher models a potential recording itself, similar to kinematic description in mechanics, then a model variable and an observable coincide.

In any measurement, the results are affected by peculiarities of an experimental technique and device parameters, external regular influences and noises. A typical procedure for acquisition of experimental data is illustrated in Fig. 6.3: an outer curve bounds a modelling object, filled circles are sensors for measured quantities and triangles are devices (amplifiers, limiters, etc.) converting sensor data into observables η_i. Even if one precisely knows how a measured signal is distorted by

the devices and makes corresponding corrections,[1] it is not possible in practice to get rid of interference (external regular or random influences).[2]

It is often feasible to suppress regular influences, while irregular ones called noises can only be reduced. Noises can be both of an external origin and inherent to an object. The former one is called *measurement* noise and the latter one is called *internal* or *dynamical* noise, since it affects the dynamics of an object. Noises are shown by the curves with arrows in Fig. 6.3. Measurement noise can be additive $\eta = f(x) + \xi$, multiplicative $\eta = f(x) \cdot \xi$ or enter the relationships between observables and model variables in a more complicated way.

The form of the function f relating observables and model variables is determined by the properties of measurement devices and transmission circuits. To avoid signal distortion, the devices must possess the following properties:

 (i) A wide enough dynamic range $U_{max} - U_{min}$ allowing to transmit both high- and low-amplitude signals without violation of proportions. For instance, a dynamic range of a device shown in Fig. 6.4 is insufficient to transmit a high-amplitude signal.

(ii) A necessary bandwidth allowing to perceive and transmit all the spectral components (Sect. 6.4.2) of an input signal in the same way and ignore "alien" frequencies. Too large a bandwidth is undesirable since more interference and noise can mix in a signal. However, its decrease is fraught with a signal distortion due to the growth in the response time τ_u to a short pulse (a characteristic of the inertial properties of a device, Fig. 6.4c). Narrow frequency band of a converting device is often used for a purposeful filtering of a signal. Preserving only "low-frequency" spectral components (low-pass filtering) leads to
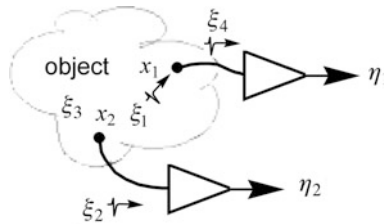

Fig. 6.3 A scheme illustrating data acquisition from an object under consideration: x_i are quantities, which characterise an object under study, and η_i are observables. *Filled circles* are sensors which send signals corrupted with noises ξ_i to measurement devices denoted by *triangles*

---

[1] For example, when e.m.f. is measured with a voltmeter, one can either allow for finiteness of R_v or use a classical no-current compensatory technique with a potentiometer (Kalashnikov, 1970, pp. 162–163; Herman, 2008) which is free of the above shortcoming.

[2] Thus, experiments show that in electric measurements (e.g., Fig. 6.2) a sensitive wideband device (e.g., a radio receiver) connected in parallel with a voltmeter or a cardiograph detects also noise, human speech and music, etc.
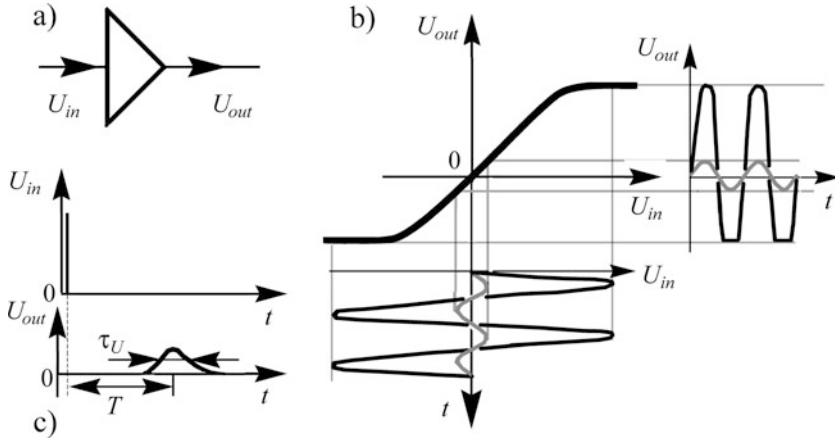
Fig. 6.4 Measurement device properties: (**a**) a device transmitting a signal; (**b**) its transfer characteristic $U_{out} = f(U_{in})$, a low-amplitude input signal (the *grey curve*) is transferred without distortions, while a high-amplitude one (the *black curve*) is limited, i.e. its peaks are cut off; (**c**) when a short pulse comes to an input of a device at a time instant $t = 0$, a response emerges at its output with a delay time T and is blurred due to finiteness of a response time τ_u

smoothing of a signal. High-pass filtering removes a constant non-zero component and slow *trends* (drifts).

(iii)   A sufficiently high sensitivity. Internal noise level of a device should be small enough to give an opportunity to distinguish an informative signal at the device output confidently.

Questions of imperfection of measurement devices and non-trivial correspondence between model variables and observables relate also to statistical data used in modelling of social processes and humanitarian problems. Distortion of those data by people and historical time may be quite significant and uncontrolled. In modelling from such data, a researcher must be especially careful, having in mind that even electric measurements with sufficiently "objective" devices and noise reduction techniques often raise doubts and require special attention.

6.1.2 How to Increase or Reduce a Number of Characterising Quantities

If available observables are regarded as components of a state vector $\mathbf{x}(t)$, their number is often insufficient for a dynamical description of an original, i.e. for a unique forecast of future states based on a current one. There are several approaches to *increasing the number of model variables D*. Some of them are justified theoretically (Takens' theorems, Sect. 10.1.1), others rely on intuition and ad hoc ideas.

The simplest and most popular way is the *time-delay embedding*. According to it, components of the vector $\mathbf{x}(t)$ are the subsequent values of a scalar observable separated by a time delay τ: $x_1(t) = \eta(t)$, $x_2(t) = \eta(t + \tau)$, ..., $x_D(t) = \eta(t + (D-1)\tau)$.

According to the *successive differentiation technique*, temporal derivatives of an observable are used as dynamical variables: $x_1(t) = \eta(t)$, $x_2(t) = \mathrm{d}\eta(t)\big/\mathrm{d}t$, ..., $x_D(t) = \mathrm{d}^{D-1}\eta(t)\big/\mathrm{d}t^{D-1}$. However, it is hardly applicable, if the measurement noise is considerable (e.g. Fig. 7.8a, b): a negligible fringe on the plot of a slightly noise-corrupted cosine function $\eta(t) = \cos t + \xi(t)$ strongly amplifies under the differentiation so that an expected sinusoidal profile on the plot $\mathrm{d}\hat{x}\big/\mathrm{d}t$ versus t is not seen at all.

Noise can be reduced to some extent if one uses integrals of an observable as dynamical variables: $x_2(t) = \int\limits_0^t \eta(t')\mathrm{d}t'$, etc. Similarly, one can get a variable expressed via subsequent values of an observable via *weighted summation* as $x_2(t) = a_0\eta(t) + a_1\eta(t-\Delta t) + a_2\eta(t-2\Delta t) + \ldots$, where a_k are weight coefficients.

One can also use a combination of all the above-mentioned approaches and other techniques to get time series of additional model variables (Sect. 10.1.2).

There are situations where the structure of a dynamical system is known, but computing the values of some dynamical variables directly from observables is impossible. Then, one speaks of "hidden" variables. In such a case, special techniques described in Sect. 8.2 may appear helpful.

In practice, it may also be necessary to reduce the number of observables if some of them do not carry information useful for modelling. It can be accomplished via the analysis of interrelations between observables and removal of the quantities, which represent linear combinations of the others. Furthermore, *dimensional and similitude methods* can be fruitful (Sena, 1977; Trubetskov, 1997): a spectacular historical example of a problem about fluid flow in a pipe, where one converts from directly measured dimensional quantities to a less number of their dimensionless combinations (similitude parameters), is considered in Barenblatt (1982).

6.2 Analogue-to-Digital Converters

To measure quantities of different nature, either constant or time-varying, one often tries to convert their values into electric voltages and currents. Electric signals can be easily transmitted from remote sensors and processed with the arsenal of standard devices and techniques. Previously, measured values were fixed by deviations of a galvanometer needle, paint traces on a plotter tape, and luminescence of an oscilloscope monitor. However, contemporary measurement systems usually represent data in a digital form with the aid of special transistor devices called *analogue-to-digital converters* (ADCs). The problem of analogue-to-digital conversion consists in the transformation of an input voltage at a measurement instant into a proportional number and, finally, in getting a discrete sequence of numbers. For a signal waveform to

be undistorted, conditions of *Kotel'nikov's theorem* must be fulfilled: A continuous signal can be restored from a discrete sequence of its values only if a sampling frequency is at least twice as large as a maximal frequency which is present in its power spectrum (Sect. 6.4.2), i.e. corresponds to a non-zero component.

The principle of ADC functioning and the reasons limiting accuracy of the resulting data are illustrated in Fig. 6.5. The scheme realises the so-called parallel approach: An input voltage is compared simultaneously with n reference voltages. The number of reference voltages and the interval between the neighbouring ones are determined by the range of measured values and the required precision, i.e. the number of binary digits in output values. For the three-digit representation illustrated in the example and allowing to record eight different numbers including zero, one needs seven equidistant reference voltages. They are formed with the aid of a resistive divider of a reference voltage U_{ref}. The latter determines an upper limit of the measured voltages and is denoted $7U$ on the scheme.

A measured voltage U_{in} is compared to the reference levels with the aid of seven comparators k_i, whose output voltages take the values which are regarded in binary system equal to

- 1 if a voltage at the contact "+" exceeds a voltage at the contact "−",
- 0, otherwise.

Thus, if a measured voltage belongs to the interval $(5U/2,\ 7U/2)$, then the comparators with numbers from 1 to 3 are set to the state "1" and the comparators from 4 to 7 to the state "0". A special logical scheme (a priority encoder) converts
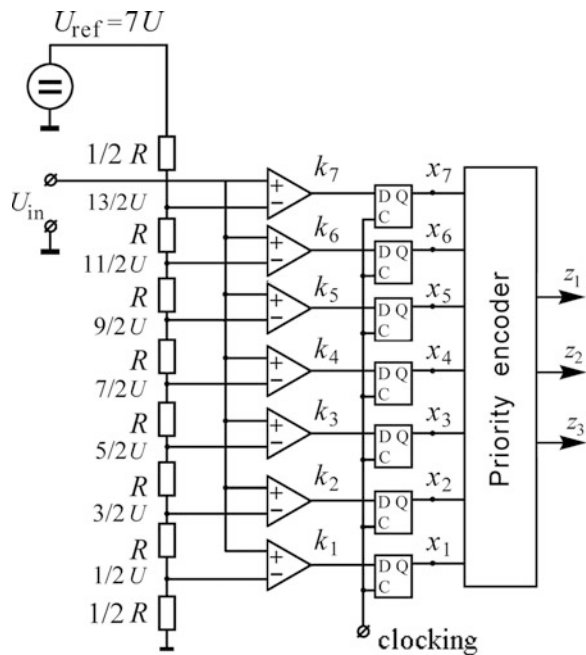

Fig. 6.5 A scheme of a three-digit ADC realising the parallel approach

those states into a binary number $z_1 z_2 z_3$ (011 in the example) or a corresponding decimal number (3 in the example). If a voltage varies in time, the priority encoder cannot be connected directly to outputs of the comparators, since it may lead to erroneous results. Therefore, one uses D triggers, shown by the squares "DQC" in Fig. 6.5, to save an instantaneous value of the voltage at outputs of the comparators and maintain it during a measurement interval. Measurement instants are dictated by a special clocking signal. If the latter is periodic, then one gets an equidistant sequence of binary numbers (a time series) at the encoder output.

The conversion of an analogue quantity into a several-digit number is characterised by a "quantisation error" equal to half an input voltage increment necessary to change the lowest order digit at the output. An eight-digit ADC has $2^8 = 256$ gradations ($\Delta x = x_{max}/256$), a 12-digit ADC has $2^{12} = 4096$ gradations ($\Delta x = x_{max}/4096$). If one performs an inverse transformation of the obtained number into a voltage with the aid of a digital-to-analogue converter, a quantisation error manifests itself as superimposed "noise". Besides, there are errors caused by the drift and non-linearity of the scheme parameters so that an overall error in the resulting observed values is determined by combinations of all the factors and indicated in a device certificate.

The parallel method for the realisation of the analogue-to-digital conversion is non-parsimonious, since one needs a separate comparator for each reference level. Thus, one needs 100 comparators to measure values ranging from 0 to 100 at a unit step. This number rises with the measurement resolution. Therefore, there have been developed and widely used approaches, which are better in this respect, e.g. *weighing* and *counting* techniques. Under the weighing technique, a result is obtained in several steps, since only a single digit of a binary number is produced at a single step. Firstly, one checks whether an input voltage exceeds a reference voltage of the highest order digit. If it does, the highest order digit is set equal to "1" and the reference voltage is subtracted from the input voltage. The remainder is compared with the next reference voltage and so on. Obviously, one needs as many comparison steps as many binary digits are contained in an output value. Under the counting technique, one counts a number of summations of the lowest order reference voltage with itself to reach an input voltage. If a maximal output value is equal to n, then one needs at most n steps to get a result. In practice, combinations of different approaches are often used.

6.3 Time Series

6.3.1 Terms

At an ADC output and in many other situations, data about a process under investigation are represented as a *finite sequence of values of an observed quantity corresponding to different time instants*, i.e. a *time series* $\eta(t_1), \eta(t_2) \dots, \eta(t_N)$, where $t_1, t_2, \dots, t_N$ are observation instants and their number N is called *time series*

length. If a value of a single scalar quantity is measured at each time instant t_i, one speaks of a *scalar* time series. It is denoted as $\{\eta(t_i)\}_{i=1}^N$ or $\{\eta_i\}_{i=1}^N$, where $\eta_i = \eta(t_i)$. If k quantities $\eta_1, \ldots, \eta_k$ (Fig. 6.3) are measured simultaneously at each instant t_i, one speaks of a *vector* time series, since those quantities can be considered as components of a k-dimensional vector $\boldsymbol{\eta}$. A vector time series is denoted similarly: $\{\boldsymbol{\eta}(t_i)\}_{i=1}^N$ or $\{\boldsymbol{\eta}_i\}_{i=1}^N$. Thus, the notation η_i is used below in two different cases: (i) a scalar time series, where i is time index; (ii) a vector observable, where i means a coordinate number. Its meaning in each concrete case is determined by context unless otherwise stated.

Elements of a time series (scalars or vectors) are also called *data points*. A number of a point i is called *discrete time*. If time intervals between subsequent observation instants t_i are the same, $t_i - t_{i-1} = \Delta t$, $i = 2, \ldots, N$, then a time series is called *equidistant*, otherwise *non-equidistant*. One also says that the values are sampled uniformly or non-uniformly in time, respectively. An interval Δt between successive measurements is called *sampling interval* or discretisation interval. For a non-equidistant series, a sampling interval $\Delta t_i = t_i - t_{i-1}$ varies in time. In practice, one deals more often with equidistant series.

To check quality of a model constructed from a time series (Sects. 7.3, 8.2.1 and 10.4), one needs another time series from the same process, i.e. a time series which was not used for model fitting. Therefore, if the data amount allows, one distinguishes two parts in a time series $\{\eta_i\}_{i=1}^N$. One of them is used for model fitting and called a *training time series*. Another one is used for diagnostic check of a model and called a *test time series*.[3]

6.3.2 Examples

Time series from different fields of practice and several problems, which are solved with the use of such data, are exemplified below. The first problem is forecast of the future behaviour of a process.

6.3.2.1 Meteorology (a Science About Atmospheric Phenomena)

At weather stations, one measures hourly values of different quantities including air temperature, humidity, atmospheric pressure, wind speed at different heights, rainfall, etc. At some stations, measurements are performed for more than 100 years. Variations in the mentioned quantities characterised by the timescales of the order of several days are ascribed to *weather* processes (Monin and Piterbarg, 1997). Weather forecast is a famous problem of synoptic meteorology.

---

[3] In the field of artificial neural networks, somewhat different terminology is accepted. A test series is a series used to compare different empirical models. It allows to select the best one among them. For the "honest" comparison of the best model with an object, one uses one more time series called a *validation time series*. A training time series is often called a *learning sample*. However, we follow the terminology described in the text above.
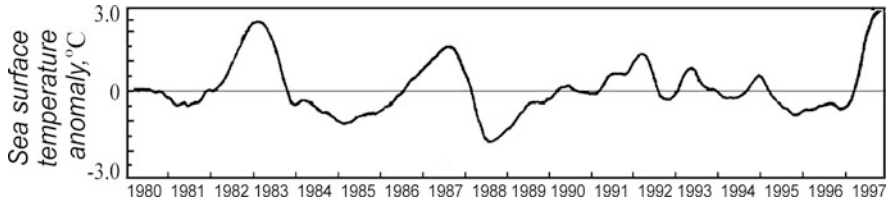
Fig. 6.6 Anomaly of sea surface temperature in eastern equatorial zone of Pacific Ocean (the values averaged over 5 months are shown). Sampling interval is $\Delta t = 1$ month (Keller, 1999)

Slower processes whose typical timescales exceed 3–4 months are called *climatic*. They are studied by *climatology*. Examples of their characteristics are sea surface temperature (a mean temperature of upper mixed layer, whose depth is about several dozens of meters, Fig. 6.6), sea level (at different coastal areas), thickness of ice, surface of ice cover, plant cover of the Earth, total monthly rainfall at a certain area, closed lakes level, etc. Besides, variations in many weather characteristics averaged over a significant time interval and/or a wide spatial area become climatic processes, e.g. mean monthly air temperature at a certain location, instantaneous value of temperature averaged over a 5° latitudinal zone, annual air temperature of the Northern Hemisphere. As for the spatial averaging, it is currently possible due to a global network of weather stations covering most of the surface of all continents. Distances between neighbouring stations are about 10–100 km.

6.3.2.2 Solar Physics

For a long time, a popular object of investigation is a time series of annual sunspot number (Fig. 6.7). This quantity is measured since telescope has been invented, more precisely, since 1610 (i.e. for almost 400 years). The process reflects magnetic activity of the Sun which affects, in particular, irradiation energy and solar wind intensity (Frik and Sokolov, 1998; Judd and Mees, 1995; Kugiumtzis et al., 1998; Yule, 1927) and, hence, leads to changes in the Earth's climate.
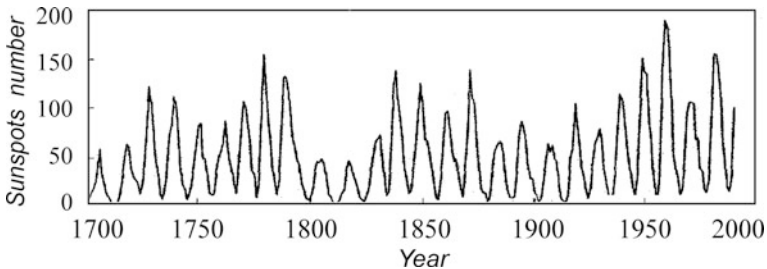

Fig. 6.7 Annual Wolf's numbers of sunspots. Sampling interval is $\Delta t = 1$ year. Eleven-year cycle of the Sun activity is noticeable

6.3.2.3 Seismology

Earthquakes occur in the block, cut by multiple ruptures, strongly non-uniform, solid shell of the Earth called lithosphere as a result of its deformation due to tectonic forces. General equations governing the process are still unknown (Sadovsky and Pisarenko, 1997). There are reasons to think that a seismic regime is affected by various physical and chemical processes including thermal, electric and others. In practice, one measures mechanical tension fields at different areas of the Earth's surface. Another form of data representation is time intervals between successive strong earthquakes $\Delta t_i = t_i - t_{i-1}$, where t_i is an instant of an ith shock. It can be interpreted as a non-equidistant time series. The values of Δt_i vary strongly between different observation areas and periods.

To study seismic activity, one uses equidistant time series as well. For instance, one measures a quantity proportional to the acceleration of the Earth's surface vibrations with the aid of seismographs (Koronovskii and Abramov, 1998).

6.3.2.4 Finance

For participants of events occurring at equity markets, it is important to be able to foresee changes in currency exchange rates, stock prices, etc. Those processes are affected by multiple factors and fluctuate quickly in a very complicated manner. Time series of currency exchange rates are often recorded at sampling interval of 1 h (and even down to 2 min). One often reports daily values of stock prices, see Figs. 6.8 and 6.9 and Box and Jenkins (1970); Cecen and Erkal (1996); Lequarre (1993); Makarenko (2003); Soofi and Cao (2002).

6.3.2.5 Physiology and Medicine

In this field, one often encounters the problem of diagnostics rather than forecast. Physiological signals reflecting activity of the heart, brain and other organs are one of the main sources of information for physicians in diagnosing. One uses electro-cardiograms (difference of potentials between different points at the chest surface, Fig. 6.10), electroencephalograms (potentials at the scalp), electrocorticograms (intracranial brain potentials), electromyograms (potentials inside muscles or on the
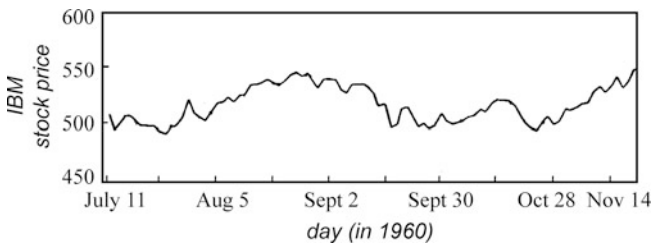

Fig. 6.8 Stock prices for the IBM company. Sampling interval $\Delta t = 1$ day; the values for the end of a day are shown (Box and Jenkins, 1970)
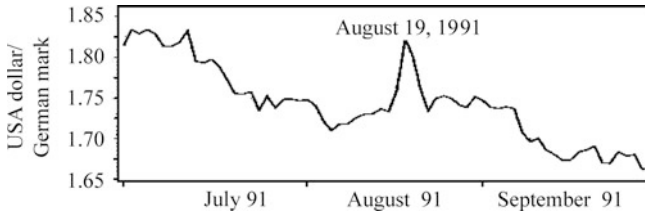
Fig. 6.9 Currency exchange rate between USA dollar and German mark in 1991 (Lequarre, 1993). Sampling interval $\Delta t = 1$ day
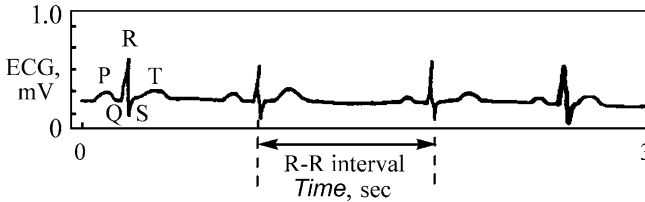

Fig. 6.10 Electrocardiogram (Rigney et al., 1993). A characteristic PQRST complex and the so-called $R – R$ *interval* are shown. Sampling interval $\Delta t = 1$ ms

skin), acceleration of finger oscillations for a stretched hand (physiological tremor), concentration of oxygen in the blood, heart rate, chest volume representing a respiration process, etc. A typical sampling interval is of the order of 1 ms.

It is important to be able to detect signs of a disease at early stages. For that, one might need quite sophisticated methods for the analysis of signals.

6.3.2.6 Transport

In this field as in many technical applications, a problem of automatic control often arises. For instance, one measures data representing simultaneously a course of a boat and a rudder turn angle (Fig. 6.11). Having those data, one can construct an automatic system allowing to make control of a boat more efficient, i.e. to reduce its wagging and fuel consumption (Ljung, 1991).
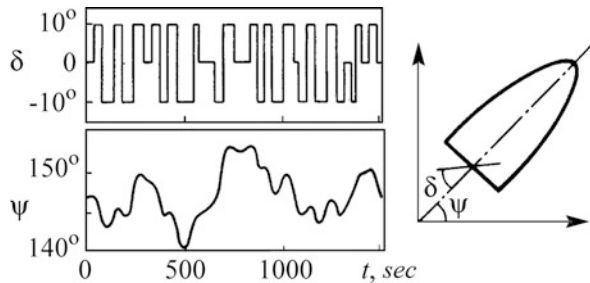

Fig. 6.11 Simultaneous time series of a rudder turn angle (random turns) and a course of a boat (Ljung, 1991). Sampling interval $\Delta t = 10$ s

6.3.2.7 Hydrodynamics

Investigation of turbulent motion in a fluid is one of the oldest and most complex problems in non-linear dynamics. Chaotic regimes are realised in experiments with fluid between two cylinders rotating in opposite directions or in a mixer with a rotating turbine inside. The data are, for instance, time series of fluid velocity at a certain spatial location measured at typical sampling interval of 1 ms (Letellier et al., 1997).

6.3.2.8 Chemistry

Considerable attention of researchers is paid to chaotic behaviour in many chemical reactions. The data from those systems are presented in the form of time realisations of reagent concentrations, e.g. Ce^{IV} ions in the Belousov and Zhabotinsky reaction (Brown et al., 1994; Letellier et al., 1998b).

6.3.2.9 Laser Physics

Observed complex behaviour of a laser under periodic pulse pumping (Fig. 6.12) can be used to estimate some parameters of the laser and further to study a dependence of those parameters on external conditions including a temperature regime. The data are a time series of irradiation intensity measured with the aid of photodiodes.

6.3.2.10 Astrophysics

In fact, the only source of information about remote objects of the Universe (stars) is time series of their irradiation intensity. Those time series are collected with the aid of radio- and optical telescopes (Fig. 6.13).

Fig. 6.12 Data from a ring laser in a chaotic regime (Hubner et al., 1993): irradiation intensity. Sampling interval $\Delta t = 40$ ns
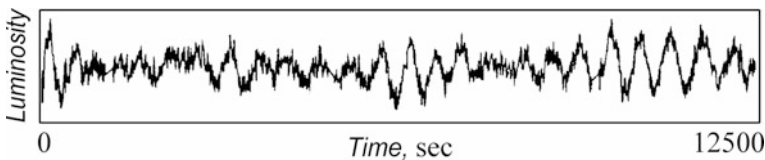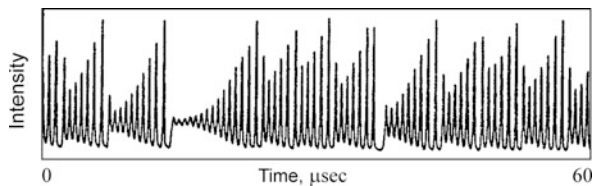

Fig. 6.13 Variations of luminance of a dwarf star PG-1159, $\Delta t = 10$ s (Clemens, 1993). The time series was recorded continuously during 231 h

The list of examples, problems and objects can be continued. Their number permanently rises. ADCs with $\Delta t = 10^{-8} - 10^{-9}$ s and data storage devices with memory sizes of hundreds of gigabytes are already easily accessible for a researcher. One still does not observe a saturation in the development of the devices for acquisition, storage and processing of time series. Even the above examples suffice to show that time realisations of motions in real-world systems are usually very complex and irregular. Yet, one now knows that complicated chaotic motions can be demonstrated even by simple non-linear dynamical systems so that the problem of modelling from a time series does not seem hopeless even though it requires a development of non-trivial techniques.

6.4 Elements of Time Series Analysis

6.4.1 Visual Express Analysis

Human capabilities to recognise visual images are so well developed that we can compete even with specialised computers in such activity. It is thought that a person gets about 70% of sensory information via the eyes. Visual analysis of data, if they are presented in a graphical form, can be very fruitful in modelling. It can give an idea about an appropriate form of model functions and kind and dimensionality of model equations. The most natural step is visual assessment of time realisations of a process $\eta(t)$, see Fig. 6.14 (left panels).

One should consider time realisations of sufficient length in order that peculiarities of motion allowing identification of a process could manifest themselves. Thus, for *periodic motions* (Fig. 6.14a), such a peculiarity is complete repeatability of a process with some period T. A motion is *quasi-periodic* (Fig. 6.14b) if there are

————————————————————————————————————→

Fig. 6.14 Time realisations of regular (**a**, **b**) and irregular (**c–h**) processes and their periodograms (formulas are given in Sect. 6.4.2). (**a**) Periodic process: variations in voltage on a semiconductor diode in a harmonically driven *RL* diode circuit (provided by Prof. E.P. Seleznev). (**b**) Quasi-periodic process: variations in voltage on a non-linear element in coupled generators with quadratic non-linearity which individually exhibit periodic self-sustained oscillations (provided by Prof. V.I. Ponomarenko). (**c**) Narrowband stationary process. (**d**) Narrowband process with non-stationarity in respect of expectation. (**e**) Narrowband process with non-stationarity in respect of variance. The data on the panels **c**, **d**, **e** are signals from an accelerometer attached to a hand of a patient with Parkinson's disease during spontaneous tremor epochs (provided by the group of Prof. P. Tass, Research Centre Juelich, Germany). (**f**) Wideband stationary process: anomaly of the sea surface temperature in Pacific ocean ($5\,°N - 5\,°S$, $170\,°W-120\,°W$), the data are available at http://www.ncep.noaa.gov. (**g**) Wideband process with non-stationarity in respect of expectation: variations in global surface temperature of the Earth. An anomaly of the GST (i.e. its difference from the mean temperature over the base period 1961–1990) is shown (Lean et al., 2005). (**h**) Wideband process with the signs of non-stationarity in respect of variance: variations in the global volcanic activity quantified by the optical depth of volcanic aerosol (Sato et al., 1993)
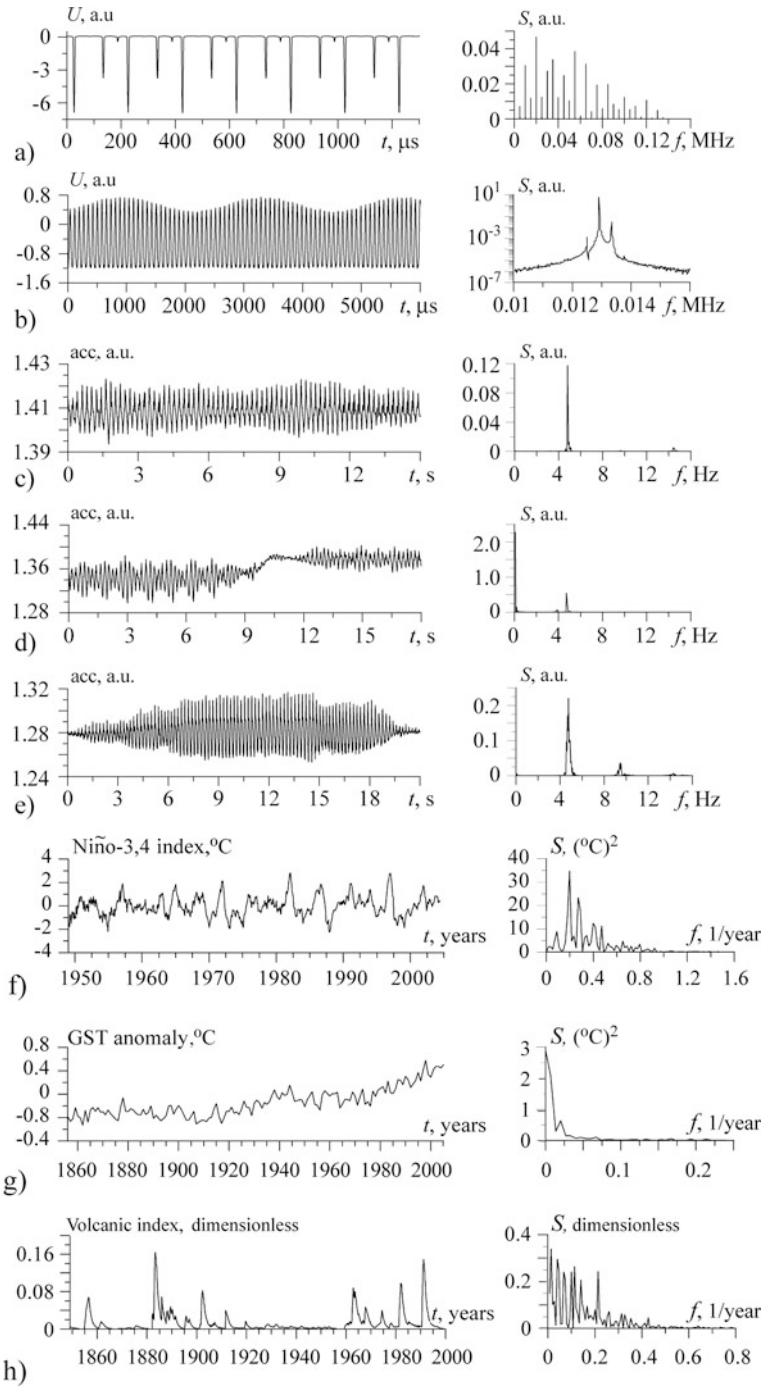
Fig. 6.14 (continued)

two or more characteristic timescales (i.e. periods of harmonic components) whose ratio T_i / T_j is an irrational number. Periodic and *quasi-periodic motions* are called *regular motions* in contrast to the cases illustrated in Fig. 6.14c–h which are depleted of obvious regularity, i.e. represent *irregular motions*.

Figure 6.14c, f shows *stationary processes* whose statistical characteristics do not change in time, while Fig. 6.14d, e, g, h shows temporal profiles looking more like *non-stationary processes* (see Sects. 4.1.3 and 6.4.4). In simple cases, non-stationary motions are recognised by eye if qualitatively or quantitatively different stages can be distinguished in their time realisations.

By considering the distance between successive maxima or minima in a time realisation and the shape of the temporal profile, one can estimate basic frequency of a signal and even a frequency range covered by its significant harmonic components (see Sect. 6.4.2). For instance, the distance between most pronounced minima is practically constant (about 200 μs) for the voltage variations shown in Fig. 6.14a; the distance between successive maxima for the accelerometer signal fluctuates stronger (Fig. 6.14c) and for the climatic process shown in Fig. 6.14f, it fluctuates much stronger. Therefore, a relative width of the peak in the power spectrum corresponding to a basic frequency is smallest for the electric signal (practically, a discrete line at 5 kHz, Fig. 6.14a), somewhat greater for the accelerometer signal (the peak at 5 Hz, Fig. 6.14c), and much greater for the climatic process (the smeared peaks at 0.2 and 0.33 1/year, Fig. 6.14f), i.e. the process in Fig. 6.14f is most wideband of these three examples. At the same time, the periodic electric signal exhibits a complicated time profile involving both flat intervals and voltage jumps (Fig. 6.14a). Therefore, its power spectrum exhibits many additional almost discrete lines at higher harmonics of the basic frequency: 10, 15, 20 kHz (an especially high peak) and so on up to 130 kHz. Non-stationarity often leads to an increase in the low-frequency components that is most clearly seen in Fig. 6.14d, g.

Another widespread approach to the visual assessment relies upon a procedure of *phase orbit reconstruction* when one shows the values of dynamical variables computed from an observable (Sects. 6.1.2 and 10.1.2) along the coordinate axes. Data points in such a space represent states of an object at successive time instants (Fig. 6.15). Possibilities of visual analysis of the phase portraits are quite limited. Without special tools, one can just consider two-dimensional projections of the phase portraits on a flat screen (Fig. 6.15b). Cycles are easily identified since they are represented by thin lines (the lower graph in Fig. 6.15b). A torus projection to a plane looks like a strip with sharp boundaries (the upper graph), which differs from a more "smeared" image of a chaotic attractor (the right graph). The pictures, which are more informative for the distinction between chaotic and quasi-periodic motions, are obtained with the aid of phase portrait sections, e.g. a stroboscopic section or a section based on the selection of extrema in the time realisations. Such a section for a torus is a closed curve (Fig. 6.15b, white line), for a cycle it is a point or several points and for a chaotic attractor it is a set of points with a complex structure. Analysis of phase portraits is more fruitful for the identification of complex non-periodic motions compared to the spectral analysis of the observed signals.
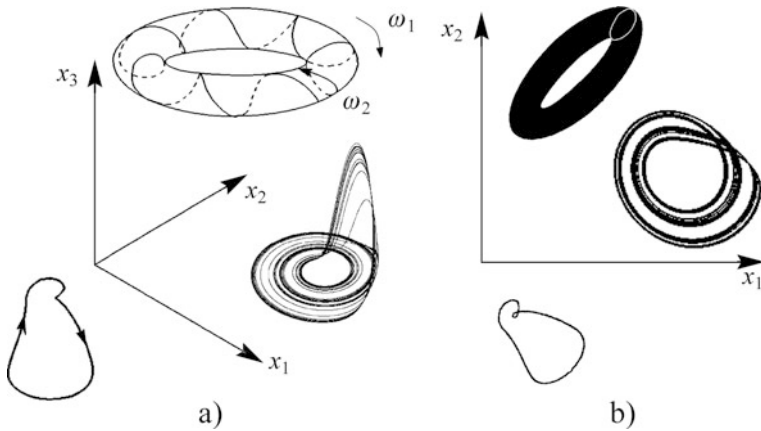
Fig. 6.15 Examples of different dynamical regimes. (**a**) Qualitative outlook of possible phase orbits in a three-dimensional phase space: a limit cycle (the *lower graph*), a torus (the *upper graph*) and a chaotic attractor (the *right graph*). (**b**) Projections to a plane representing typical pictures on an oscilloscope screen. The white line on the black background denote a projection of a two-dimensional section of the portrait

6.4.2 Spectral Analysis (Fourier and Wavelet Transform)

Most often, the term "spectral analysis" refers to Fourier transform, i.e. decomposition of a signal into harmonic components. However, in a generalised sense, spectral analysis is a name for any representation of a signal as a superposition of some *basis* functions. The term "spectrum" refers then to a set of those functions (components). Below, we briefly consider a traditional *Fourier analysis* and a more novel and "fashion" tool called *wavelet analysis* which is very fruitful, in particular, to study non-stationary signals.

6.4.2.1 Fourier Transform and Power Spectrum

This topic is a subject of multitude of books and research papers. It underlies such fields of applied mathematics as spectral analysis (Jenkins and Watts, 1968) and digital filters (Hamming, 1983; Rabiner and Gold, 1975). We only briefly touch on several points.

Firstly, let us recall that according to Weierstrass' theorem, any function $\eta = F(t)$ continuous on an interval $[a,b]$ with $F(a) = F(b)$ can be arbitrarily accurately represented by a trigonometric polynomial. The idea is readily realised in time series analysis. If a time series is equidistant and contains an even number of points N, sampling interval is Δt, $a = t_1$, $b = a + N \cdot \Delta t = t_N + \Delta t$, then one can show that an original signal $\{\eta(t_i)\}_{i=1}^{N}$ for all observation instants can be uniquely represented as the sum:

$$\eta(t_i) = a_0 + \sum_{k=1}^{N/2} a_k \cos(k\omega t_i) + \sum_{k=1}^{N/2-1} b_k \sin(k\omega t_i), \ i = 1, \dots, N, \qquad (6.1)$$

where

$$\omega = \frac{2\pi}{b-a} = \frac{2\pi}{N\Delta t}.$$

Coefficients of the trigonometric polynomial (6.1) are expressed via the formulas

$$a_0 = \frac{1}{N} \sum_{i=1}^{N} \eta_i, \, a_{N/2} = \frac{1}{N} \sum_{i=1}^{N} (-1)^i \eta_i, \qquad (6.2)$$

$$a_k = \frac{2}{N} \sum_{i=1}^{N} \eta_i \cos(k\omega t_i), k = 1, \dots, N/2 - 1, \qquad (6.3)$$

$$b_k = \frac{2}{N} \sum_{i=1}^{N} \eta_i \sin(k\omega t_i), k = 1, \dots, N/2 - 1. \qquad (6.4)$$

The formulas (6.2), (6.3) and (6.4) converting the values of η_i into the coefficients a_k and b_k are called the direct *discrete Fourier transform* (DFT). The formula (6.1) providing calculation of η_i from a_k and b_k is called the inverse DFT.

Based on these transforms, one can construct an approximate description of an original signal, in particular, smooth it. For instance, higher frequencies corresponding to big values of k often reflect noise influence so that it is desirable to get rid of them. It can be accomplished in the simplest way if one zeros the corresponding coefficients a_k and b_k and performs the inverse DFT (6.1). Thereby, one gets a more gradually varying ("smoother") signal. This is a kind of a low-pass filter. A high-pass filter can be realised in a similar way by zeroing coefficients corresponding to small values of k. To get a band-pass filter, one zeros all the coefficients outside of a certain frequency band. These simple versions of digital filters are not the best ones (Hamming, 1983; Rabiner and Gold, 1975).

One can often get a sufficiently good approximation to a continuous function $F(t)$ over a finite interval with the aid of a trigonometric polynomial. At that, even trigonometric polynomials of quite a high order can be used, while the use of high-order algebraic polynomials leads to significant troubles (Sect. 7.2.3). If a function $F(t)$ is periodic, it can be approximated well by a trigonometric polynomial over the entire number axis. We stress that the trigonometric system of functions is especially useful and has no "competitors" for approximation of periodic functions.

Physical Interpretation as Power Spectrum

The mean-squared value of an observable η is proportional to physical power if η is an electric voltage or a current in a circuit. One can show that this mean-squared

value is equal to the sum of the mean-squared values of the terms in the right-hand side of Eq. (6.1). In other words, the power is distributed *among frequencies*:

$$\frac{1}{N} \sum_{i=1}^{N} \eta_i^2 = \sum_{k=0}^{N/2} S_k, \tag{6.5}$$

where S_k is a power contained in a harmonic component with a frequency $k\omega$: $S_k = (a_k^2 + b_k^2)/2$ for $1 \leq k < N/2$ and $S_k = a_k^2$ for $k = 0, N/2$. Physically, an observed signal may represent a superposition of signals from several sources. If each of those sources demonstrates harmonic oscillations with its own frequency, then its intensity in the observed signal is reflected by the values of S_k at the corresponding frequency. The quantities S_k allow to detect different sources of oscillations and estimate their relative intensity. If each frequency corresponding to a considerable value of S_k is related to oscillations of a certain harmonic oscillator, then the number of considerable components is equal to the *number of degrees of freedom* involved in the process. Since the total power in a signal is represented as a set (spectrum) of components according to Eq. (6.5), the set of S_k is called "power spectrum" of the process $\eta(t)$. Strictly speaking, this is only an estimate of the power spectrum (see below).

The concept of the power spectrum is so easily defined only for a deterministic periodic function $\eta(t)$ with a period $2\pi/\omega$, since such a function is uniquely represented by a trigonometric Fourier series:

$$\eta(t) = a_0 + \sum_{k=1}^{\infty} [a_k \cos(k\omega t) + b_k \sin(k\omega t)], \tag{6.6}$$

whose coefficients are, in general, non-zero and expressed via the integrals of the original function $\eta(t)$.

However, even in this case, one must take into account that a finite set of coefficients in Eq. (6.1) obtained via the direct DFT from a time series is only an approximation to the theoretical spectrum. If the most part of the power is contained in relatively low frequencies (but higher than $\omega = 2\pi/(N\Delta t)$), then such an approximation is sufficiently accurate. Widely known is a phenomenon of frequency mimicry (masking) which is following. A model (6.1) includes maximal frequency of $\omega N/2 = \pi/\Delta t$, which is called Nyquist frequency. The period of the corresponding harmonic component is equal to the doubled sampling interval. Any components with the frequencies exceeding the Nyquist frequency would be linear combinations of the basis functions in Eq. (6.1) over the set of the observation instants t_i. If such components are introduced into a model, then the lower frequencies must be excluded to provide linear independence of the basis functions. In other words, higher frequency components cannot be distinguished from the combinations of the lower frequency components, e.g. $\cos\left((N/2 + k)\, j\omega\Delta t\right) = \cos(\pi j + k\omega j\Delta t) = (-1)^j \cos(jk\omega\Delta t)$, where $k > 0$ and $t_j = j\Delta t$. It looks as if the former were masked by the latter.

The situation gets even more complex in the case of a non-periodic function $\eta(t)$. Such a function cannot be accurately represented by the series (6.6) over the entire number axis. However, under certain conditions (integrability over the entire number axis and smoothness), one can write down a similar representation in the form of the Fourier integral, i.e. replace discrete frequencies $k\omega$ in Eq. (6.6) by the continuous range of values:

$$\eta(t) = \int_0^\infty A(\omega)\cos(\omega t)\mathrm{d}\omega + \int_0^\infty B(\omega)\sin(\omega t)\mathrm{d}\omega, \tag{6.7}$$

$$A(\omega) = \frac{1}{\pi}\int_{-\infty}^\infty \eta(t)\cos(\omega t)\mathrm{d}t, \;\; B(\omega) = \frac{1}{\pi}\int_{-\infty}^\infty \eta(t)\sin(\omega t)\mathrm{d}t. \tag{6.8}$$

The transforms (6.7) and (6.8) are called *continuous Fourier transforms* (the inverse and direct transforms, respectively). The above discrete transforms are their analogues. The energy[4] in a signal $\eta(t)$ is expanded into a continuous *energy spectrum* as $\int_{-\infty}^\infty \eta^2(t)\mathrm{d}t = \int_0^\infty E(\omega)\mathrm{d}\omega$, where $E(\omega) = A^2(\omega) + B^2(\omega)$.

Finally, let us consider the case where $\eta(t)$ is a realisation of a stationary random process. Typically, it is almost always non-periodic. Moreover, integrals (6.8) almost always do not exist, i.e. one cannot define A and B even as random quantities. Spectral contents of a process are then described via the *finitary Fourier transform*, i.e. for $\eta(t)$ over an interval $[-T/2, T/2]$ one gets

$$A_T(\omega) = \frac{1}{\pi}\int_{-T/2}^{T/2} \eta(t)\cos(\omega t)\mathrm{d}t, \; B_T(\omega) = \frac{1}{\pi}\int_{-T/2}^{T/2} \eta(t)\sin(\omega t)\mathrm{d}t. \tag{6.9}$$

Further, one computes expectations of A_T, B_T and defines *power spectrum* as

$$S(\omega) = \lim_{T\to\infty} \frac{\left\langle A_T^2(\omega) + B_T^2(\omega)\right\rangle}{T}, \tag{6.10}$$

where angular brackets denote the expectation. The quantity on the left-hand side of (6.10) is power, since it represents energy divided by the time interval T. In this case, the values of S_k obtained with DFT are random quantities. The set of such values is a rough estimate of the power spectrum. In particular, it is not a consistent estimator since the probability density function for each S_k is proportional to that for the χ^2 distribution with two degrees of freedom so that the standard deviation of

---

[4] Not a power. Mean power equals zero in this case, since a signal must decay to zero at infinity to be integrable over the entire number axis.

S_k equals its mean and does not decrease with increasing time series length (Brockwell and Davis, 1987; Priestley, 1989). This set is called *periodogram* if all the components are multiplied by N, i.e. if one converts from power to energy. Several examples are presented in Fig. 6.14 (the right panels). To get an estimator with better statistical properties, it is desirable to average S_k over several realisations of the process or to "smooth" a single periodogram (Brockwell and Davis, 1987; Priestley, 1989).

Importance of the power spectrum concept is related to the fact that behaviour of many real-world systems in the low-amplitude oscillatory regimes is adequately described with harmonic functions. Such dynamical regimes are well known and understood in detail. They are observed everywhere in practice and widely used in technology, e.g. in communication systems. Linear systems (filters, amplifiers, etc.) are described in terms of the transfer functions, i.e. their basic characteristic is the way how the power spectrum of an input signal is transformed into the power spectrum of the output signal. The phase spectrum which is a set of initial phases of the harmonic components in Eq. (6.1) is also often important. Multiple peculiarities of the practical power spectrum estimation and filtering methods are discussed, e.g., in Hamming (1983), Jenkins and Watts (1968), Press et al. (1988), Rabiner and Gold (1975) and references therein.

An Example: Slowly Changing Frequency Contents and Windowed DFT

It is a widespread situation when a signal under investigation has a time-varying power spectrum. One of the simplest examples is a sequence of two sinusoidal segments with different frequencies:

$$\eta(t) = \begin{cases} \sin 2t, & -\pi \le t < 0, \\ \sin 4t, & 0 \le t < \pi. \end{cases} \tag{6.11}$$

We performed the analysis over the interval $[-\pi, \pi]$ from a time series of the length of 20 data points with the sampling interval $\Delta t = \pi/10$ and $t_1 = -\pi$ (Fig. 6.16a).

The signal can be described well with a trigonometric polynomial (6.1) containing many considerable components (Fig. 6.16a). However, more useful information can be obtained if the signal is divided into two segments (windows) and a separate trigonometric polynomial is fitted to each of them (Fig. 6.16b). This is a so-called windowed Fourier transform. In each window, one gets a spectrum consisting of a single significant component that makes physical interpretation of the results much easier. The windowed DFT reveals that frequency contents of the signal changes in time that cannot be detected with a single polynomial (6.1). Non-stationary signals are often encountered in practice and can be analysed with the windowed DFT. However, there exists a much more convenient contemporary tool for their analysis called "wavelet transform".
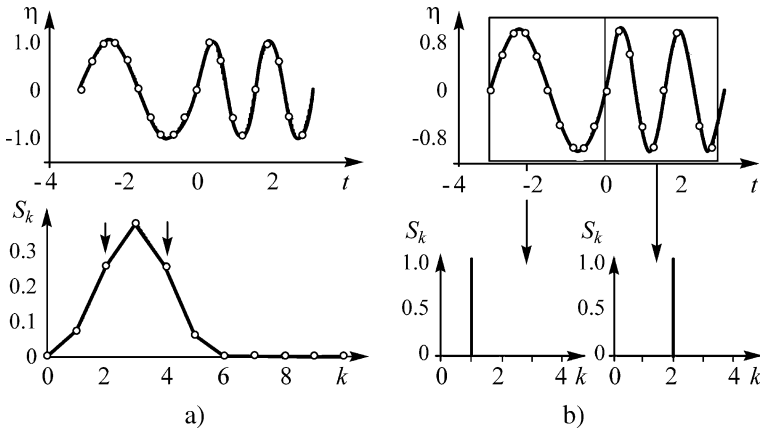
Fig. 6.16 An example of a non-stationary signal: (**a**) two segments of a sinusoid and a superimposed plot of an approximating trigonometric polynomial (6.1). Power spectrum contains five significant components (the *bottom panel*). *Arrows* indicate frequencies of the two original sinusoidal segments; (**b**) analogous plots for the windowed DFT. There is a single non-zero component in each spectrum. Their frequencies correspond to the values of k twice as small as in the *left panel* since the number of points in each window is twice as small as in the original time series

6.4.2.2 Wavelet Transform and Wavelet Spectrum

A very efficient approach to the analysis of functions $\eta = F(t)$ exhibiting pulses, discontinuities, breaks and other singularities is to use basis functions $\phi_k(t)$ called wavelets, which are well localised both in time and frequency domains. They have become an extremely popular tool during the last 20 years (see, e.g., the reviews Astaf'eva, 1996; Koronovskii and Hramov, 2003; Torrence and Compo, 1998 and references therein).

The term "wavelet" has been introduced in 1984 and become widely used. Many researchers call wavelet analysis "mathematical microscope" (Astaf'eva, 1996). Here, we do not go into strict mathematical definitions and explain only some basic points. Wavelet is a function $\phi(t)$, which

(i) is well localised both in time domain (it quickly decays when $|t|$ rises) and frequency domain (its Fourier image is also well localised);

(ii) has zero mean $\int_{-\infty}^{\infty} \phi(t)\mathrm{d}t = 0$;

(iii) satisfies a scaling condition (a number of its oscillations does not change under variations in the timescale).

An example is the so-called DOG-wavelet[5] shown in Fig. 6.17:

$$\phi(t) = \mathrm{e}^{-t^2/2} - 0.5\mathrm{e}^{-t^2/8}. \tag{6.12}$$

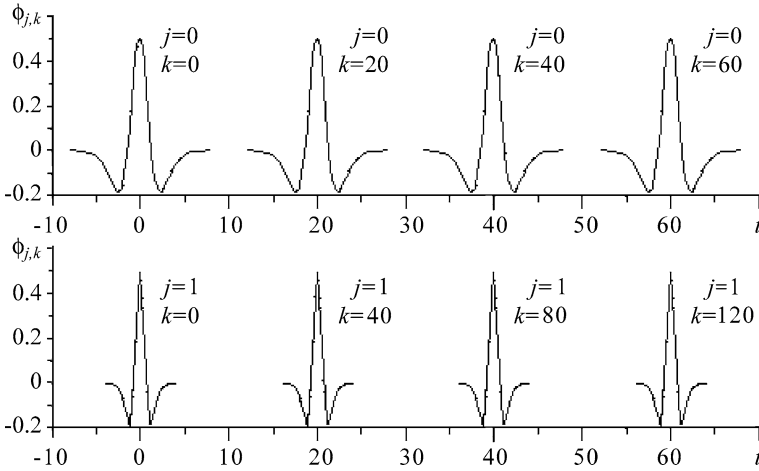[5] Difference of Gaussians, i.e. Gauss functions.

Fig. 6.17 An example of wavelet and construction of the set of basis functions via shifts (from *left* to *right*) and compressions (from *top* to *bottom*). Normalisation is not taken into account

Based on a certain wavelet function, one can construct a set of functions via its shifts and scaling transformations (compression and stretching along the t-axis). The functions obtained are conveniently denoted by two subscripts:

$$\phi_{j,k}(t) = 2^{j/2}\phi\left(2^j t - k\right), \quad -\infty < j, k < \infty, \tag{6.13}$$

where j and k are integers. Increasing j by 1 changes the scale along the time axis twice (compression of the function plot), while increasing k by 1 shifts the plot of the function $\phi_{j,k}$ by $k/2^j$ along the t-axis (Fig. 6.17). The normalising multiplier $2^{j/2}$ is introduced for convenience to preserve constant norm of $\phi_{j,k}$, i.e. the integrals of squared functions are all equal: $\|\phi_{j,k}\|^2 = \|\phi\|^2$.

The constructed set of the localised functions $\phi_{j,k}$ covers the entire t-axis due to shifts, compression and stretching. Under a proper choice of $\phi(t)$, the set is a basis in the space of functions, which are square summable over the entire axis. Strictly speaking, $\phi(t)$ is called wavelet only in this case (Astaf'eva, 1996). The condition is fulfilled for a wide class of functions including that presented in Fig. 6.17. Basis functions $\phi_{j,k}$ are often called wavelet functions. Since all of them are obtained via the transformations of $\phi(t)$, the latter is often called "mother wavelet".

Examples of mother wavelet are very diverse (Fig. 6.18). Numerical libraries include hundreds of them (http://www.wavelet.org). A widely used one is the complex *Morlet wavelet*

$$\phi(t) = \pi^{-1/4}e^{-t^2/2}(e^{-i\omega_0 t} - e^{-\omega_0^2/2}), \tag{6.14}$$

where ω_0 determines the number of its oscillations over the decay interval and the second term in parentheses is introduced to provide zero mean. Real part of the Morlet wavelet is shown in Fig. 6.18 for $\omega_0 = 6$.
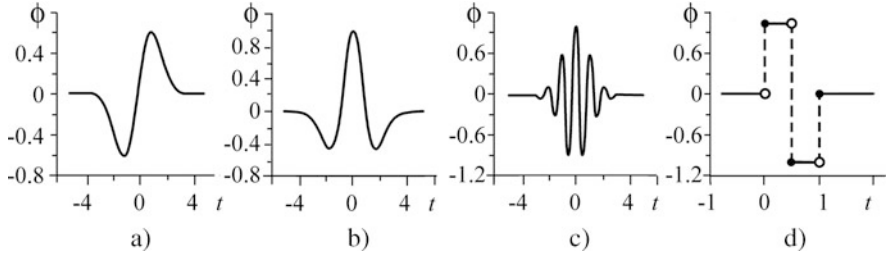
Fig. 6.18 Examples of wavelets: (**a**) WAVE wavelet; (**b**) "Mexican hat"; (**c**) Morlet wavelet (a real part); (**d**) HAAR wavelet

To construct an approximating function for a time series, one should select a finite number of terms from the infinite set of functions $\phi_{j,k}$. Wavelet-based approximation can be vividly illustrated with an example of *HAAR wavelet* (Fig. 6.18d) (Misiti et al., 2000). Let us consider an equidistant time series of length $N = 2^m$, where m is a positive integer, $\Delta t = 1/N$, $t_1 = 0$. As a set of basis functions, it is convenient to use the following functions from the entire set $\phi_{j,k}$ supplemented with a constant:

$$
\begin{aligned}
& 1, \\
& \phi_{0,0}(t) \equiv \phi(t), \\
\phi_{1,0}(t) \equiv \phi(2t), \quad & \quad \phi_{1,1}(t) \equiv \phi(2t - 1) \\
\phi_{2,0}(t) \equiv \phi(4t), \; \phi_{2,1}(t) \equiv \phi(4t - 1), \; \phi_{2,2}(t) & \equiv \phi(4t - 2), \; \phi_{2,3}(t) \equiv \phi(4t - 3), \\
& \cdots, \\
\phi_{m-1,0}(t) \equiv \phi(2^{m-1}t), \quad \cdots, \quad & \phi_{m-1,2^{m-1}-1}(t) \equiv \phi(2^{m-1}t - 2^{m-1} + 1).
\end{aligned}
$$
(6.15)

An original time series is precisely represented as the sum

$$
\eta_i = c_0 + \sum_{j=0}^{m-1} \sum_{k=0}^{2^j - 1} c_{j,k} \phi_{j,k},
$$
(6.16)

Coefficients corresponding to the terms with $j = m - 1$ depend only on the difference of the observed values at neighbouring time instants, i.e. on the oscillations with the period $2\Delta t$ corresponding to the Nyquist frequency. Since those functions describe only the smallest scale variations, the sum of them

$$
D_1(t_i) = \sum_{k=0}^{2^{m-1}-1} c_{m-1,k} \phi_{m-1,k}(t_i),
$$
(6.17)

is said to describe the *first-level details*. The remaining component

$$A_1(t_i) = \eta_i - D_1(t_i) = c_0 + \sum_{j=0}^{m-2} \sum_{k=0}^{2^j-1} c_{j,k} \phi_{j,k}, \qquad (6.18)$$

is called the *first-level approximation*. The first-level approximation no longer contains variations with a period $2\Delta t$ (Fig. 6.19). Similarly, one can determine details in the first-level approximation and so on, which is realised via the basis functions with smaller j (Fig. 6.19). A general definition of the nth-level details and nth-level approximation is introduced analogously to Eqs. (6.17) and (6.18): details $D_n(t_i)$ are small-scale components of a signal and approximations $A_n(t_i)$ are larger scale components. Approximation of the last mth level is just a mean value of an original signal. Finally, an original signal is equal to the sum of its mean value and all details: $\eta_i = A_m(t_i) + D_m(t_i) + D_{m-1}(t_i) + \cdots + D_1(t_i)$.

The value of j determines the scale of the consideration: the greater the j, the smaller the scale. The value of k specifies a temporal point of consideration. To continue an analogy between a wavelet and a microscope, one can say that k is a focusing point, j determines its magnification and the kind of the mother wavelet is responsible for its "optical properties".

If only a small number of the wavelet coefficients $c_{j,k}$ appear significant, then the rest can be neglected (zeroed). Then, the preserved terms give a parsimonious and sufficiently accurate approximation to an original signal. In such a case, one says that the wavelet provides a compression of information since several wavelet coefficients can be stored instead of many values in the time series. If necessary, one can restore an original signal from those coefficients only with a small error. Wavelets are efficient to "compress" signals of different character, especially pulse-like ones. To compress signals, one can also use algebraic or trigonometric polynomials, but the field of wavelet applications appears much wider in practice (see, e.g., Frik and Sokolov, 1998; Misiti et al., 2000; http://www.wavelet.org).

Wavelet Analysis

Non-trivial conclusions about a process can be extracted from the study of its wavelet coefficients. This is a subject of the wavelet analysis in contrast to approximation and restoration of signal, which are the problems of synthesis. Above, we spoke of the *discrete wavelet analysis* since the subscripts j and k in the set of wavelet functions took discrete values. More and more careful interest is now paid to the *continuous wavelet analysis* when one uses continuous-valued "indices" of shift and scale (Astaf'eva, 1996; Koronovskii and Hramov, 2003; Torrence and Compo, 1998). The integral (continuous) *wavelet transform* of a signal $\eta(t)$ is defined by the expression

$$W(s,k) = \frac{1}{\sqrt{s}} \int_{-\infty}^{\infty} \eta(t) \cdot \phi\left(\frac{t-k}{s}\right) dt \equiv \int_{-\infty}^{\infty} \eta(t) \cdot \phi_{s,k}(t) \, dt, \qquad (6.19)$$
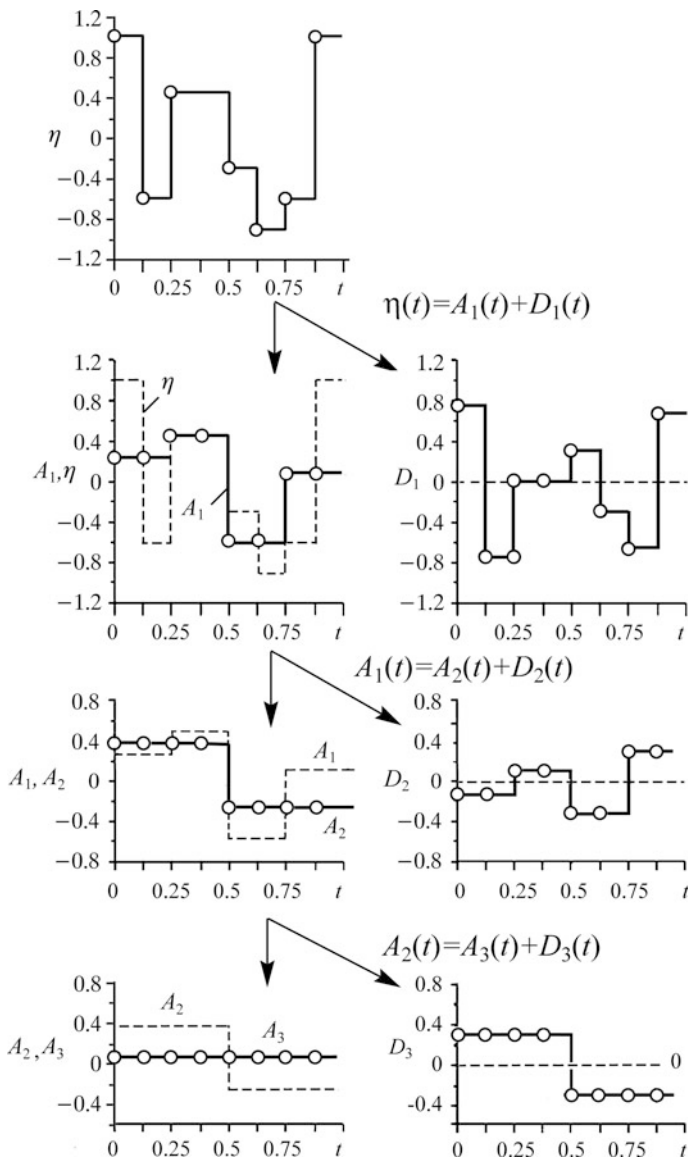
Fig. 6.19 Wavelet transform: approximations and details at various levels

where s and k are real numbers (continuous-valued parameters of scale and shift), wavelet functions are denoted as $\phi_{s,k}(t) = (1/\sqrt{s})\,\phi\left((t-k)/s\right)$ and the parameter s is analogous to 2^{-j} in the discrete transform (6.13). The bivariate function $W(s,k)$ is called the *wavelet spectrum* of the signal $\eta(t)$. It makes vivid physical sense. A big value of $|W(s_1,k_1)|$ indicates that signal variations with the timescale s_1 around the time instant k_1 are intensive. Roughly speaking, the value of $|W(s,k_1)|$

at fixed k_1 shows frequency contents of the signal around the time instant k_1. If the values corresponding to small s are large, then small-scale (high-frequency) components are present. The values of $|W(s_1, k)|$ at fixed s_1 show how the intensity of the signal component corresponding to the timescale s_1 changes in time. Thus, the wavelet spectrum carries information both about frequency contents of the signal and its temporal localisation in contrast to the Fourier-based power spectrum, which provides information only about the frequency contents without any temporal localisation. Therefore, the wavelet spectrum is also called a time – frequency spectrum.

The *wavelet spectrum* satisfies "energy condition", which allows one to relate it to a decomposition of the signal energy in time and frequency domains:

$$\int_{-\infty}^{\infty} \eta^2(t)\mathrm{d}t = \frac{1}{C_\phi} \int_{-\infty}^{\infty} \int_{-\infty}^{\infty} W^2(s, k)\frac{\mathrm{d}s\,\mathrm{d}k}{s^2}, \qquad (6.20)$$

where C_ϕ is a normalising coefficient depending on the kind of the mother wavelet. If the value of W^2 is integrated over time k, one gets a function of the timescale, which is called *global energy spectrum* or *scalogram*:

$$E_W(s) = \int_{-\infty}^{\infty} W^2(s, k)\mathrm{d}k. \qquad (6.21)$$

It can be used for the global characterisation of the signal frequency contents along with the periodogram. Scalogram is typically a more accurate estimator of the power spectrum. It resembles a smoothed periodogram (Astaf'eva, 1996; Torrence and Compo, 1998).

A wavelet spectrum can be visualised as a surface in a three-dimensional space. More often, one uses a contour map of $|W(s, k)|$ or a two-dimensional map of its values on the plane (k, s) in greyscale, e.g., where the black colour denotes large values and the white colour indicates zero values. Of course, only an approximate computation of the integral (6.19) is possible in practice. To do it, one must specify a signal behaviour outside an observation interval $[a,b]$ (often, a signal is simply zeroed) that introduces artificial peculiarities called edge effects. How long intervals at the edges should be ignored depends on the mother wavelet used and on the timescale under consideration (Torrence and Compo, 1998). Let us illustrate performance of the wavelet analysis for the temporal profile shown in Fig. 6.20a: two sinusoidal segments with different frequencies (similar examples are considered, e.g., in Koronovskii and Hramov, 2003). DOG wavelet is used for a time series of the length of 1000 points over an interval $[-\pi, \pi]$ and zero padding outside the interval. The global Fourier-based spectrum does not reveal the "structure of non-stationarity". The wavelet spectrum clearly shows the characteristic timescales (Fig. 6.20b). In particular, it allows to distinguish low-frequency oscillations at the beginning of the time series; black spots correspond to the locations of the sinusoid
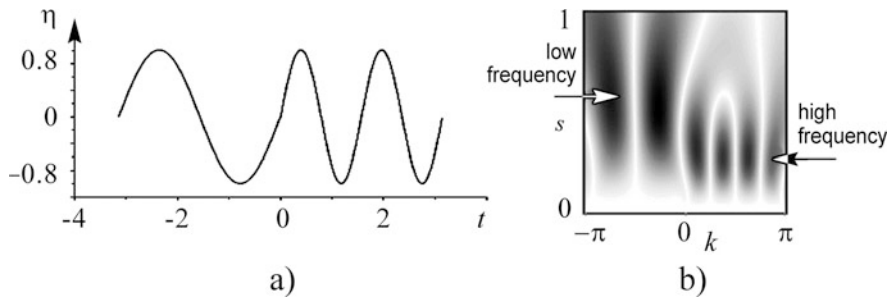
Fig. 6.20 Wavelet analysis: (**a**) two sinusoidal segments with different frequencies; (**b**) wavelet spectrum obtained with the aid of DOG wavelet

extrema and "instantaneous" period. Edge effects (which are, indeed, strong for a signal containing so small number of oscillations with a characteristic period) are not taken into account here for the sake of illustration simplicity.

Additional examples are given in Fig. 6.21 which presents wavelet spectra of the time series given in Fig. 6.14. For the computations, we have used the Morlet wavelet (6.14) with $\omega_0 = 6$. Edge effects for this wavelet function at the timescale s cover intervals of the width $s\sqrt{2}$ (Torrence and Compo, 1998). One can clearly see the basic periods as dark horizontal lines in Fig. 6.21a–e. Moreover, Fig. 6.21a exhibits additional structure related to the complicated temporal profile, which is seen in Fig. 6.14a. Decrease in the oscillation amplitude during the change in the mean value in Fig. 6.14d (the interval from the 9th to the 12th s) is reflected as a white "gap" in the horizontal black line in Fig. 6.21d. Figure 6.21e clearly shows the increase in the oscillation amplitude in the beginning and its decrease in the end. Figure 6.21h shows higher volcanic activity during the periods 1890–1910 and 1970–1990. One can see complicated irregular structures in Fig. 6.21f, g. Still, a characteristic timescale of about 60 months (5 years) can be recognised in Fig. 6.21f.

The wavelet analysis is extremely useful for the investigation of non-stationary signals containing segments with qualitatively different behaviour. It is efficient for essentially non-uniform signal (pulse-like, etc.) and signals with singularities (discontinuities, breaks, discontinuities in higher order derivatives), since it allows to localise singularities and find out their character. The wavelet spectrum exhibits a characteristic regular shape for fractal signals (roughly speaking, strongly jagged and self-similar signals): such signs appear inherent to many real-world processes. Moreover, one can analyse spatial profiles in the same way, e.g., the Moon relief (Misiti et al., 2000) exhibits a very complex shape with different scales related to the bombardment of the Moon with meteorites of various sizes. Wavelets are applied to data analysis in geophysics, biology, medicine, astrophysics and information processing systems, to speech recognition and synthesis, image compression, etc. Huge bibliography concerning wavelets can be found, e.g., in Astaf'eva (1996), Koronovskii and Hramov (2003), Torrence and Compo (1998) and at the website (http://www.wavelet.org).
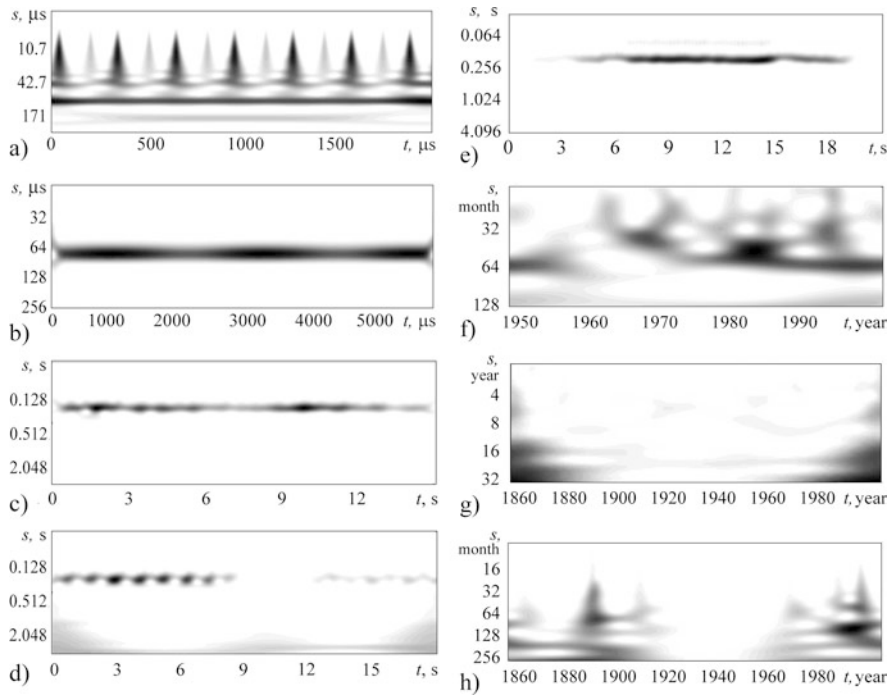
Fig. 6.21 Wavelet spectra for the signals shown in Fig. 6.14: (**a**) periodic electric signal (voltage on a diode); (**b**) quasi-periodic electric signal (voltage on a non-linear element); (**c**) stationary accelerometer signal; (**d**) non-stationary accelerometer signal in respect of the expectation; (**e**) non-stationary accelerometer signal in respect of the variance; (**f**) stationary climatic process (Niño-3.4 index); (**g**) non-stationary climatic process in respect of the expectation (variations in the global surface temperature); (**h**) non-stationary climatic process in respect of the variance (volcanic activity)

6.4.3 Phase of Signal and Empirical Mode Decomposition

It is very fruitful in multiple situations to consider a *phase of a signal*. Here, we discuss contemporary concepts of the phase. Roughly speaking, this is a variable characterising repeatability in a signal. It rises by 2π between any two successive maxima. Especial role of this variable is determined by its high sensitivity to weak perturbations of a system. Changes in the amplitude may require significant energy, while a phase can be easily changed by a weak "push".[6]

The term "phase" is often used as a synonym of the words "state" or "stage". In Sect. 2.1.3, we have discussed a state vector and a state space of a dynamical system and spoken of a phase orbit drawn by a state vector. The meaning of

---

[6] Thus, a phase of a pendulum oscillations (Fig. 3.5a) can be changed by holding it back at a point of maximal deflection from an equilibrium state without energy consumption.

the term "phase" is different in the field of signal processing. Thus, the phase of a harmonic signal $x(t) = A \cos(\omega t + \phi_0)$ is an argument of the cosine function $\phi = \omega t + \phi_0$. The phase ϕ determines the value of the cosine function. However, to specify a state completely, one needs to know the amplitude A as well, i.e. the phase is not a complete characteristic of a state. Apart from $\phi = \omega t + \phi_0$ called "unwrapped phase" (Fig. 6.22b, the upper panel), one uses a "wrapped" phase $\phi(t) = (\omega t + \phi_0) \bmod 2\pi$ defined only over the interval $[0, 2\pi)$ (Fig. 6.22b, the lower panel). The latter approach makes sense, since the values of the unwrapped phase differing by 2π correspond to the same states, the same values of the cosine function.

A vivid geometrical interpretation of the introduced concept of phase is possible if one represents a signal $x(t) = A \cos(\omega t + \phi_0)$ as a real part $\operatorname{Re} z(t)$ of a complex-valued signal $z(t) = A \mathrm{e}^{\mathrm{i}(\omega t + \phi_0)}$. Then, a vector $z(t)$ on the plane (x, y), where $x(t) = \operatorname{Re} z(t)$ and $y(t) = \operatorname{Im} z(t)$, rotates uniformly with a frequency ω along a circle of radius A centred at the origin (Fig. 6.22a). Its phase $\phi = \omega t + \phi_0$ is a rotation angle of $z(t)$ relative to the positive direction of the x-axis. To compute an unwrapped phase, one takes into account a number of full revolutions. Thus, such a phase is increased by 2π after each revolution. For a harmonic signal, it rises linearly in time at a speed equal to the angular frequency of oscillations. A plot of the wrapped phase is a piecewise linear function (a saw), Fig. 6.22b.

The concept of the phase originally introduced only for a harmonic signal was later generalised to more complicated situations. The most well-known and widespread generalisation to the case of non-harmonic signals is achieved via construction of an *analytic signal* (Gabor, 1946). The latter is a complex-valued signal, whose Fourier image has non-zero components only at positive frequencies. From an original signal $x(t)$, one constructs an analytic signal $z(t) = x(t) + \mathrm{i}y(t)$, where $y(t)$ is the *Hilbert transform* of $x(t)$:
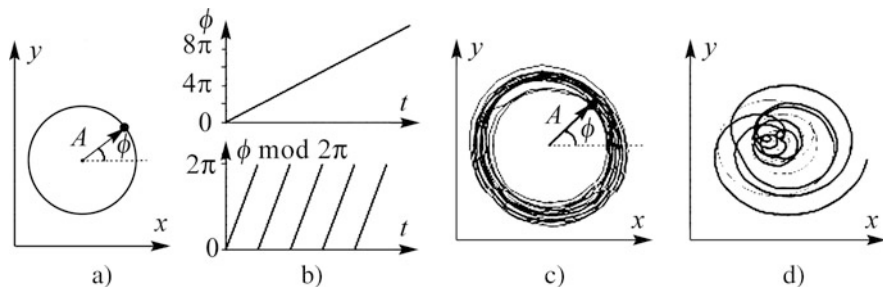
Fig. 6.22 Phase definition: (**a**) an orbit on the plane (x, y) for a harmonic signal $x(t)$, y is the Hilbert transform of x, A and ϕ are its amplitude and phase, respectively; (**b**) unwrapped and wrapped phases of a harmonic signal versus time; (**c**) an orbit on the complex plane for a non-harmonic narrowband signal, its amplitude and phase introduced through the Hilbert transform are shown; (**d**) the same illustration for a wideband signal, whose phase is ill-defined

$$y(t) = \text{P.V.} \int_{-\infty}^{\infty} \frac{x(t')\mathrm{d}t'}{\pi(t - t')}, \qquad (6.22)$$

P.V. denotes the Cauchy principal value of the improper integral. The phase is defined as an argument of the complex number z, i.e. as a rotation angle of the radius vector on the plane (x, y). This approach is widely used in radio-physics and electrical engineering (Blekhman, 1971, 1981; Pikovsky et al., 2001). For a harmonic signal $x(t) = A\cos(\omega t + \phi_0)$, the conjugated signal is $y(t) = \sin(\omega t + \phi_0)$ and the phase coincides with the above definition. For an "almost sinusoidal" signal, one observes rotation of the vector z not strictly along a circle but "almost" along a circle (Fig. 6.22c). The phase increases on average at the speed equal to the mean angular frequency of the oscillations.

The phase makes clear physical sense for oscillatory signals with a pronounced main rhythm (Anishchenko and Vadivasova, 2004; Pikovsky et al., 2001). For complicated irregular signals, an analytic signal constructed via the Hilbert transform may not reveal a rotation about a well-defined centre (Fig. 6.22d). Then, the above formal definition of the phase is, as a rule, useless. However, if the observed signal is a combination of a relatively simple signal from a system under investigation and a superimposed interference, then one can try to extract a simpler signal and determine its phase as described above. Let us consider two basic approaches to the extraction of a simple signal: band-pass filtering and empirical mode decomposition.

6.4.3.1 Band-pass Filtering

The simplest approach is to use a band-pass filter (Sect. 6.4.2), which let pass only components from a small neighbourhood of a certain selected frequency. If the frequency band is not wide, then one gets a signal with a pronounced main rhythm, whose phase is easily defined via the Hilbert transform (Fig. 6.22c). However, what frequency band should be used? Does a filtered signal relate to the process under investigation or is it just an artificial construction? One can answer such questions only taking into account additional information about the system under investigation. On the one hand, the frequency band should not be too narrow: In the limit case, one gets a single sinusoid whose phase is well defined but does not carry any interesting information. On the other hand, the frequency band should not be too wide, since then there would not be a rotation of the vector z about a single centre, i.e. repeatability to be described by the phase would not exist.

Another widespread opportunity to get an analytic signal is a complex wavelet transform (Lachaux et al., 2000):

$$z(t) = \frac{1}{\sqrt{s}} \int_{-\infty}^{\infty} x(t')\Phi^* \left(\frac{t' - t}{s} \right) \mathrm{d}t' \qquad (6.23)$$

at a fixed timescale s realised with the Morlet wavelet (6.14): $\Phi(t) = \pi^{-1/4}\left[\exp(-i\omega_0 t) - \exp\left(-\omega_0^2/2\right)\right]\exp(-t^2/2)$. This is equivalent to the band-pass filtering of an original signal with the subsequent application of the Hilbert transform. Namely, the frequency band is of the width $\Delta f/f = 1/4$ and centred at the frequency $f \approx 1/s$ at $\omega_0 = 6$. Edge effects are less prominent under the use of the wavelet transform (6.23) than for many other ways of filtering.

6.4.3.2 Empirical Mode Decomposition

Apart from linear filtering, one can use other options. A technique for the decomposition of a signal into the so-called "empirical modes" recently introduced in Huang et al. (1998) has become more and more popular during the last years. This is a kind of adaptive non-linear filtering. The phase of each empirical mode is readily defined, e.g., as a variable linearly rising by 2π between subsequent maxima or via the Hilbert transform. For that, each "mode" should be a zero-mean signal whose maxima are positive and minima are negative, i.e. its plot $x(t)$ inevitably intersects the abscissa axis $(x = 0)$ between each maximum and minimum of a signal. The technique is easily implemented and does not require considerable computational efforts. A general algorithm is as follows:

  (i) To find all extrema in a signal $x(t)$.
 (ii) To interpolate between the minima and get a lower envelope $e_{\min}(t)$. For instance, the neighbouring minima can be interconnected by straight line segments (linear interpolation). Analogously, an upper envelope $e_{\max}(t)$ is obtained from the maxima of a signal.
(iii) To compute the mean $m(t) = (e_{\max}(t) + e_{\min}(t))/2$.
 (iv) To compute the so-called details $d(t) = x(t) - m(t)$. The meaning of the term is analogous to that used in the wavelet analysis (Sect. 6.4.2). The quantity $m(t)$ is called a *remainder*.
  (v) To perform the steps (i)–(iv) for the obtained details $d(t)$ and get new details $d(t)$ and a new remainder $m(t)$ (sifting procedure) until they satisfy two conditions: (1) the current remainder $m(t)$ is close to zero as compared with $d(t)$, (2) the number of extrema in $d(t)$ equals the number of its zeroes or differs from it by 1. One calls the resulting details $d(t)$ an "empirical mode" $f(t)$ or an "intrinsic mode function".
 (vi) To compute a remainder, i.e. the difference between a signal and an empirical mode $m(t) = x(t) - f(t)$. To perform the steps (i)–(v) for the remainder $m(t)$ instead of the original signal $x(t)$. The entire procedure is stopped if $m(t)$ contains too few extrema.

The process is illustrated in Fig. 6.23 with a signal representing a sum of a sinusoid and two periodic signals with triangular profiles and different periods. The period of the first triangle wave is greater than that of the sinusoid and the period of the second triangle wave is less than that of the sinusoid. As a result of the above procedure, the original signal is decomposed into the sum of three components
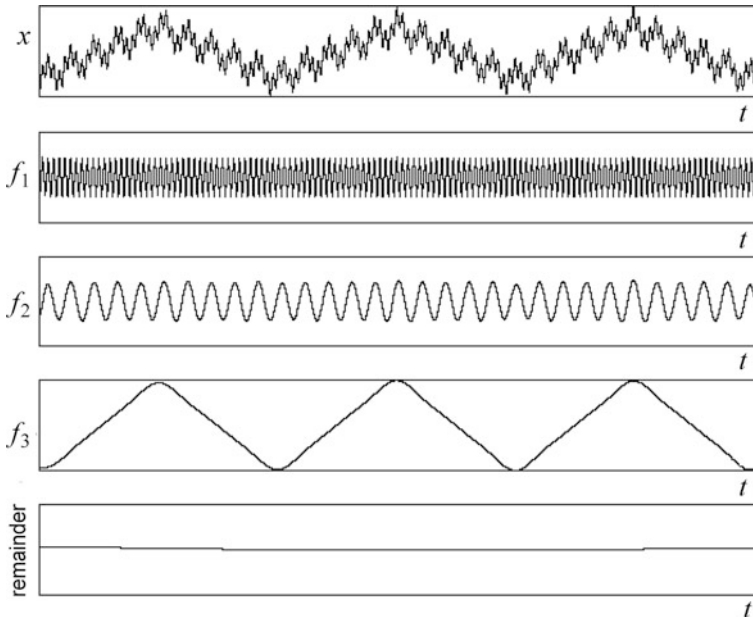
Fig. 6.23 Empirical mode decomposition (Huang et al., 1998). The *upper panel* shows an original signal. The next three panels show empirical modes. The first of them is a periodic triangular wave with a small period, the second one is a sinusoid and the third one is a triangular wave with larger period. The *lowest panel* shows a remainder, which exhibits a single extremum

(empirical modes) and a remainder, which is close to zero. An advantage of this technique over band-pass filtering is its adaptive character: it distinguishes modes based on the properties of a signal without the use of a *pre-selected* frequency band. In particular, it is more efficient in coping with non-stationary signals.

6.4.4 Stationarity Analysis

In general, *stationarity* of a process with respect to some property means constancy of that property in time. Definitions of wide-sense and narrow-sense stationarity are given in Sect. 4.1.3. Besides such a statistical stationarity related to the constancy of the distribution laws or their moments, one singles out dynamical stationarity, meaning constancy of an evolution operator (see also Sect. 11.1).

Majority of time series analysis techniques are based on the assumption of stationarity of an investigated process. However, multitude of real-world signals, including physiological, financial and others, look non-stationary. The latter results from processes, whose characteristic timescales exceed an observation time, or external events, which lead to changes in dynamics, e.g. adaptation in biological systems. Many characteristics calculated from a non-stationary time series appear meaningless or unreliable.

A lot of efforts were devoted to the problem of testing for stationarity. Previously, if *non-stationarity* was detected, a time series was rejected as useless for any further analysis or divided into segments sufficiently short to be considered as quasi-stationary. Later, many authors started to use information about the character of non-stationarity to study a process. There are situations when temporal variations in the properties of a process represent the most interesting contents of a time series. For instance, a purpose of electroencephalogram analysis is often to detect changes in the brain state. Such changes occur between different stages of sleep, between epileptic seizures and normal brain activity, and so on.

To check a process for stationarity based on a time series more or less reliably, the length of the time series must significantly exceed all timescales of interest. If components with characteristic timescales of the order of a time series length are present, then a process is typically recognised as non-stationary. However, a process may often be regarded stationary even if a time series length is considerably less than characteristic timescales of slow processes in a system. For instance, heart rate of a human being under relaxed conditions is as a rule homogeneous over time intervals of the order of several minutes. However, longer segments of data reveal new peculiarities arising due to slow biological rhythms. Since a usual 24-h electrocardiogram recording covers just a single cycle of a circadian (daily) rhythm, it is more difficult to consider it as stationary than longer or shorter recordings.

To detect non-stationarity, one uses the following basic approaches:

(i) Computation of a certain characteristic in moving window, i.e. in subsequent segments of a fixed length (it looks like a window for the consideration moves along the time axis). If the characteristic changes weakly and does not exhibit pronounced trends, then a time series is regarded stationary with respect to that characteristic, otherwise it is non-stationary. Examples of non-stationarity with respect to mean and variance are shown in Fig. 6.14d, e, g, h. In statistics there have been developed special techniques to test for stationarity with respect to the mean (Student's *t*-test, a non-parametric shift criterion, inversion criterion), the variance (Fisher's criterion, scattering criterion) and univariate distribution functions (Wilcoxon test) (Kendall and Stuart, 1979; Pugachev, 1979, 1984; von Mises, 1964). Based on the theory of statistical hypotheses testing, one may deny stationarity with respect to those characteristics at a given significance level (i.e. with a given probability of random error).

(ii) Comparison of characteristics in different time windows. One uses such characteristics as different statistical measures (criteria of χ^2, Cramer and Mises, Kolmogorov and Smirnov) (Kendall and Stuart, 1979; von Mises, 1964) and non-linear dynamics measures [cross-correlation integral (Cenis et al., 1991), cross-prediction error (Schreiber, 1997, 1999), distance between vectors of a dynamical model coefficients (Gribkov and Gribkova, 2000)]. Some approaches of such type are illustrated in Sect. 11.1.

One more recent approach, which often appears useful for the treatment of non-stationary signals (e.g. to detect drifts of parameters), is based on the analysis

of *recurrences* in a reconstructed phase space (Facchini et al., 2005; Kennel, 1997; Rieke et al., 2002). *Recurrence plot* widely used in the *recurrence analysis* (Eckmann et al., 1987) is a diagram which shows time instants of close returns of an orbit to different states of a system. It is a very convenient tool to visualise a dynamical structure of a signal. Furthermore, recurrences in the space of model coefficients may be used to directly characterise non-stationarity and select quasi-stationary intervals of an observed signal (Sect. 11.1). Recurrence plots were introduced in Eckmann et al. (1987) and extended in many works, see the dissertation (Marwan, 2003) and the review (Marwan et al., 2007) for a detailed consideration. It is also worthwhile to note that the recurrence analysis extends possibilities of estimating dimensions, Lyapunov exponents and other dynamical invariants of a system (Marwan et al., 2007), which can be used in empirical modelling to select a model structure and validate a model.

6.4.5 Interdependence Analysis

Above, we have considered techniques for a scalar time series analysis. If one observes a vector time series, e.g., simultaneous measurements of two quantities $x(t)$ and $y(t)$, then opportunities to address new questions emerge. It is often important to reveal interdependence between $x(t)$ and $y(t)$ to get ideas about the presence and character of coupling between sources of the signals. Such information can be used in modelling as well. Thus, if there is a unique relationship between $x(t)$ and $y(t)$, then it is sufficient to measure only one of the quantities, since the other one does not carry new information. If there is certain interdependence, which is not unique, then it is reasonable to construct a model taking into account interaction between two sources of signals.

There are different approaches to the analysis of interdependencies. Historically, the first tools were *cross-correlation* and *cross-spectral analysis*. They are developed within the framework of mathematical statistics and attributed to the so-called linear time series analysis. *Cross-covariance function* is defined as covariance (Sect. 4.1.2) of x and y at time instants t_1 and t_2:

$$K_{x,y}(t_1, t_2) = E\left[(x(t_1) - E[x(t_1)])\,(y(t_2) - E[y(t_2)])\right]. \qquad (6.24)$$

For a stationary case, it depends only on the interval between the time instants:

$$K_{x,y}(\tau) = E\left[(x(t) - E[x])\,(y(t + \tau) - E[y])\right]. \qquad (6.25)$$

According to the terminology accepted mainly by mathematicians, normalised cross-covariance function is called *cross-correlation function* (CCF). The latter is a *correlation coefficient* between x and y. For a stationary case, the CCF reads

$$k_{x,y}(\tau) = \frac{E\left[(x(t) - E[x])\,(y(t + \tau) - E[y])\right]}{\sqrt{\mathrm{var}[x]\mathrm{var}[y]}}, \qquad (6.26)$$

where var[x] and var[y] are the variances of the processes $x(t)$ and $y(t)$. It always holds true that $-1 \leq k_{x,y}(\tau) \leq 1$. An absolute value of $k_{x,y}(\tau)$ reaches 1 in case of deterministically linear dependence $y(t+\tau) = \alpha\, x(t) + \beta$, while $k_{x,y}(\tau) = 0$ for statistically independent processes $x(t)$ and $y(t)$. However, if the processes are related uniquely, but non-linearly, then the CCF can be equal to zero (e.g., for $y(t) = x^2(t)$ and symmetric distribution of x about zero) and "overlooks" the presence of interdependence. Therefore, one says that the CCF *characterises a linear dependence* between signals. To estimate the CCF, one uses a usual formula for an empirical moment (Sect. 2.2.1).

There are multiple modifications and generalisations of the CCF. Thus, to characterise an interdependence between components of signals at a given frequency, rather than a total interdependence, one uses cross-spectral density and coherence (a normalised cross-spectral density). However, the estimation of the cross-spectrum and coherence is connected to greater difficulties compared to the estimation of an individual power spectrum (Bloomfield, 1976; Brockwell and Davis, 1987; Priestley, 1989). DFT-based estimators analogous to the periodogram estimator of the power spectrum have even worse estimation properties compared to the latter due to an estimation bias (Hannan and Thomson, 1971), observational noise effects (Brockwell and Davis, 1987), large estimation errors for the phase spectrum at small coherence (Prietley, 1989), etc. (Timmer et al., 1998). Cross-wavelet analysis further generalises characterisation of an interdependence by decomposing it in the time – frequency domain (Torrence and Compo, 1998). Analogous to the cross-spectrum and Fourier coherence, the cross-wavelet spectrum and wavelet coherence are estimated with greater difficulties, compared to the individual wavelet power spectrum (Maraun and Kurths, 2004).

To reveal non-linear dependencies, one uses generalisations of the correlation coefficient including Spearman's index of cograduation (Kendall and Stuart, 1979), correlation ratio (Aivazian, 1968; von Mises, 1964), mutual information function (Fraser and Swinney, 1986) and others.

The corresponding approaches are developed in non-linear dynamics along two directions. The first idea is to analyse mutual (possibly, non-linear) dependencies between state vectors $\mathbf{x}(t)$ and $\mathbf{y}(t)$ reconstructed from a time series via time-delay embedding or in other way (Sects. 6.1.2 and 10.1.2). The techniques rely upon the search for nearest neighbours in state spaces (Arnhold et al., 1999; Pecora et al., 1995) or construction of mutual predictive models (Schiff et al., 1996; Schreiber, 1999). If there is a unique dependence between simultaneous values of the state vectors $\mathbf{x}(t) = \mathbf{F}(\mathbf{y}(t))$, one speaks of *generalised synchronisation* (Rulkov et al., 1995; Pecora et al., 1995; Boccaletti et al., 2002). Fruitful approaches to quantification and visualisation of non-linear interrelations from observed data are based on the recurrence analysis (Sect. 6.4.4) and include cross-recurrence plots (Groth, 2005; Marwan and Kurths, 2002, 2004; Zbilut et al., 1998) and joint recurrence plots (Marwan et al., 2007).

The second idea is to analyse *only* the phases of observed signals. Since the phase is a very sensitive variable, an interaction between oscillatory systems often manifests itself as an interdependence between their phases, while the amplitudes may

remain uncorrelated. If for two coupled self-sustained oscillators their unwrapped phase difference is constant $\phi_x(t) - \phi_y(t) = \text{const}$, then one says that *phase synchronisation* takes place. This is a thresholdless phenomenon, i.e. it can be observed for arbitrarily weak coupling between systems if their own oscillation frequencies are arbitrarily close to each other (Afraimovich et al., 1989; Pikovsky et al., 2001) and noise is absent. If even weak noise is present, then the phase difference cannot be strictly constant and one considers a softened condition $\left|\phi_x(t) - \phi_y(t) - \text{const}\right| < 2\pi$. This is definition of 1:1 synchronisation. There also exists a higher order *m:n* synchronisation defined by the condition $\left|m\phi_x(t) - n\phi_y(t) - \text{const}\right| < 2\pi$. For a considerable noise level, even the softened condition of the phase difference boundedness can be fulfilled only over a finite time interval. Then, one speaks of an effective synchronisation if that time interval significantly exceeds oscillation periods of both systems.

One introduces different numerical characteristics of phase interdependence often called *coefficients of phase synchronisation*. The most widespread among them is the so-called *mean phase coherence* (it has several names):

$$R_{m,n} = \sqrt{\left\langle \cos\left(m\phi_x(t) - n\phi_y(t)\right)\right\rangle^2 + \left\langle \sin\left(m\phi_x(t) - n\phi_y(t)\right)\right\rangle^2}, \qquad (6.27)$$

where angle brackets denote temporal averaging. It is equal to unity when the phase difference is constant (phase synchronisation) and to zero when each system exhibits oscillations with its own frequency independently of the other one. In the case of non-strict (e.g. due to noise) phase locking, the quantity $R_{m,n}$ can take an intermediate value and characterise a "degree of interdependence" between the phases. An example of efficient application of such a phase analysis to a medical diagnostic problem is given in Pikovsky et al. (2000).

In Chap. 12 and 13, we describe several techniques allowing to reveal and characterise "directional couplings" and their applications.

6.5 Experimental Example

This chapter is devoted to techniques and problems emerging at the starting stage of the modelling procedure and to acquisition and preliminary analysis of a time series (see Fig. 5.1). Instead of a summary, where we could say that probability of successful modelling rises with the amount and accuracy of prior knowledge about an object, let us discuss a real-world example of data acquisition and modelling. An object is a familiar circuit discussed above: a source of e.m.f. and resistors connected to it (Fig. 6.2a, b). However, a semiconductor sample (InSb, antimonide of indium) is included into it instead of the resistor R_v.[7] Under the room temperature, InSb is a conductor; therefore, experiments are carried out in liquid nitrogen at its boiling

---

[7] This narrow-band-gap semiconductor characterised by a large mobility of charge carriers is promising in respect of the increase in the operating speed of semiconductor devices.

Fig. 6.24 Experimental set-up: (**a**) the scheme; (**b**) the current I via a sample versus the voltage U on a sample
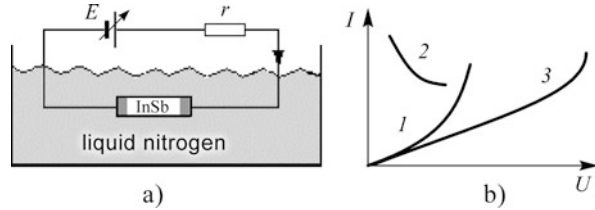
temperature of $-77\,°C$ (Fig. 6.24). Despite seeming simplicity of the object (at least, in comparison with living systems), we have selected it for an illustration due to diversity of its possible motions, mathematical tools needed for their description and difficulties in data acquisition depending on the modelling purposes.

What complexity can one expect from an oblong piece of a substance with two contacts connected to a source of constant e.m.f.? Depending on experimental conditions and exploited devices, one can observe diversity of processes ranging from a trivial direct current to oscillations at ultrahigh frequencies and even irradiation in the millimetre range of wavelengths. Registering of processes with characteristic frequencies ranging from 1 to 10^{12} Hz requires usage of different devices and analogue-to-digital converters. Moreover, starting from frequencies of about several gigahertz, digitising and, hence, modelling from time series are still technically impossible. Further, mathematical modelling of different phenomena mentioned above requires application of various tools ranging from algebraic equations to partial differential equations.

Under low voltages U at the contacts of the sample, it behaves like a usual resistor, i.e. one observes a direct current I and processes are appropriately modelled by an algebraic relationship, i.e. Ohm's law $I = U/R$, where R is a parameter meaning the resistance of the sample. The characterising quantities U and I are easily measured and can serve as observables. Linearity of their interdependence is violated with the rise in U due to the heating of the sample, whose conductance then rises as seen from the branch 1 of the characteristic (Fig. 6.24b).

With further increase in I and the heating intensity, boiling of the liquid transits from the bubble-boiling to the film[8]-boiling regime. This is reflected by the branch 2 on the dependency of the mean current on the mean voltage. Moreover, this is accompanied by the transition of the system "sample – source of e.m.f. – cooling liquid" to an oscillatory regime. Its characteristic frequencies range from less than 1 Hz to radio frequencies (dozens of kilohertz to several megahertz). Thus, one can use an ADC to record a time series. Oscillations at lower frequencies are determined by the arousal of multitude of bubbles at the surface, while higher frequencies are determined by the reactivity of the wires connected to the negative resistance of

---

[8] Liquid nitrogen in a thermos is under boiling temperature. At a low heat flow from the sample, small bubbles arise at its surface. They cover the entire surface at a more intensive heating. Thus, a vapour film is created, which isolates the sample from the cooling liquid.

the sample. Those phenomena can be modelled with stochastic differential equations. Yet, such a model contains quantities which are not directly related to the observables: heat flow from the sample, temperature dependence of its conductance, reactivity of the feed circuit.

A situation which is even more complex for observations and modelling arises if one tries to decrease heating influence and turns from a continuous power supply to a pulse regime when the voltage on the sample is supplied only during a short interval so that it has enough time to be cooled considerably until the next pulse. At that, without heat destruction of the sample and change in the boiling regime, one can achieve the voltages (the branch 3 in Fig. 6.24b) sufficient for a shock breakdown to start at local areas of the sample and created "pieces" of plasma to become a source of microwave radiation. To observe such processes, one needs a special equipment and microwave receivers, while the use of the current $I(t)$ and the voltage $U(t)$ as observables gets inefficient. The reason is that it is not clear how characterising quantities entering a DE-based model of the above oscillatory mechanism are related to such observables. More appropriate model variables would be the field strength in the sample and the concentration of the charge carriers. It is important to take into account a dependence of the drift velocity on the field strength and so on. An example of differential equations modelling such a dynamical regime is given in Bezruhcko and Erastova (1989). A more detailed modelling of the considered seemingly simple system requires to use non-linear partial differential equations.

This example cannot be regarded as an exclusive one in practice.

References

Afraimovich, V.S., Nekorkin, V.I., Osipov, G.V., Shalfeev, V.D.: Stability, structures, and chaos in nonlinear synchronisation networks. Gor'ky Inst. Appl. Phys. RAS, Gor'ky, (in Russian) (1989)

Aivazian, S.A.: Statistical Investigation of Dependencies. Metallurgiya, Moscow, (in Russian) (1968)

Anishchenko, V.S., Vadivasova, T.Ye.: Relationship between frequency and phase characteristics of chaos: two criteria of synchronization. J. Commun. Technol. Electron. **49**(1), 69–75 (2004)

Arnhold, J., Lehnertz, K., Grassberger, P., Elger, C.E.: A robust method for detecting interdependences: application to intracranially recorded EEG. Physica D. **134**, 419–430 (1999)

Astaf'eva N.M.: Wavelet analysis: basic theory and some applications. Phys. Uspekhi. **39**, 1085–1108 (1996)

Barenblatt, G.I.: Similarity, Self-similarity, Intermediate Asymptotics, Gidrometeoizdat, Leningrad (1982). Translated into English: Scaling, Self-Similarity, and Intermediate Asymptotics. Cambridge University Press, Cambridge (1996)

Bezruhcko, B.P., Erastova, E.N.: About possibility of chaotic solutions in model of narrow-band-gap semiconductor in ionisation by collision regime. Sov. Phys. *Semicon*duct. **23**(9), 1707–1709 (in Russian), (1989)

Blekhman, I.I.: Synchronisation in Nature and Technology. Nauka, Moscow (1981). Translated into English: ASME Press, New York (1988)

Blekhman, I.I.: Synchronisation of Dynamic Systems. Nauka, Moscow, (in Russian) (1971)

Bloomfield, P.: Fourier Analysis of Time Series: An Introduction. Wiley, New York (1976)

Boccaletti, S., Kurths, S., Osipov, G., Valladares, D., Zhou, C.: The synchronization of chaotic systems. Phys. Rep. **366**, 1–52 (2002)

Box, G.E.P., Jenkins, G.M.: Time Series Analysis. Forecasting and Control. Holden-Day, San Francisco (1970)

Brockwell, P.J., Davis, R.A.: Time Series: Theory and Methods. Springer, Berlin (1987)

Brown, R., Rulkov, N.F., Tracy, E.R.: Modeling and synchronizing chaotic systems from experimental data. Phys. Lett. A. **194**, 71–76 (1994)

Cecen, A.A., Erkal, C.: Distinguishing between stochastic and deterministic behavior in high frequency foreign exchange rate returns: Can non-linear dynamics help forecasting? Int. J. Forecasting. **12**, 465–473 (1996)

Čenis, A., Lasiene, G., Pyragas, K.: Estimation of interrelation between chaotic observable. Phys. D. **52**, 332–337 (1991)

Clemens, J.C.: Whole Earth telescope observations of the white dwarf star PG 1159-035 (data set E). In: Gerschenfeld, N.A., Weigend, A.S. (eds.) Time Series Prediction: Forecasting the Future and Understanding the Past. SFI Studies in the Science of Complexity, Proc. V. XV, pp. 139–150. Addison-Wesley, New York (1993)

Eckmann, J.-P., Kamphorst, S.O., Ruelle, D.: Recurrence plots of dynamical systems. Europhys. Lett. **5**, 973–977 (1987)

Facchini, A., Kantz, H., Tiezzi, E.: Recurrence plot analysis of nonstationary data: the understanding of curved patterns. Phys. Rev. E. **72**, 021915 (2005)

Fraser, A.M., Swinney, H.L.: Independent coordinates for strange attractors from mutual information. Phys. Rev. A. **33**, 1131–1140 (1986)

Frik, P., Sokolov, D.: Wavelets in astrophysics and geophysics. Computerra, vol. 8. Available at http://offline.computerra.ru/1998/236/1125/ (in Russian) (1998)

Gabor, D.: Theory of communication. J. Inst. Elect. Eng. (London). **93**, 429–459 (1946)

Gribkov, D., Gribkova, V.: Learning dynamics from nonstationary time series: analysis of electroencephalograms. Phys. Rev. E. **61**, 6538–6545 (2000)

Groth, A.: Visualization of coupling in time series by order recurrence plots. Phys. Rev. E. **72**, 046220 (2005)

Hamming, R.W.: Digital Filters, 2nd edn. Prentice-Hall, Englewood Cliffs, NJ (1983)

Herman, S.L.: Delmar's Standard Textbook of Electricity. Delmar Publishers, San Francisco (2008)

Huang, N.E., Shen, Z., Long, S.R.: The empirical mode decomposition and the Hilbert spectrum for nonlinear and non-stationary time series analysis. Proc. R. Soc. Lond. A. **454**, 903–995 (1998)

Hubner, U., Weiss, C.-O., Abraham, N.B., Tang, D.: Lorenz-like chaos in $NH_3 - FIR$ lasers (data set A). In: Gerschenfeld, N.A., Weigend, A.S. (eds.) Time Series Prediction: Forecasting the Future and Understanding the Past. SFI Studies in the Science of Complexity, Proc. V. XV, pp. 73–104. Addison-Wesley, New York (1993)

Jenkins, G., Watts, D.: Spectral Analysis and Its Applications. Holden-Day, New York (1968)

Judd, K., Mees, A.I. On selecting models for nonlinear time series. Phys. D. **82**, 426–444 (1995)

Kalashnikov, S.G.: Electricity. Nauka, Moscow, (in Russian) (1970)

Keller, C.F.: Climate, modeling, and predictability. Phys. D. **133**, 296–308 (1999)

Kendall, M.G., Stuart, A.: The Advanced Theory of Statistics, vols. 2 and 3. Charles Griffin, London (1979)

Kennel, M.B.: Statistical test for dynamical nonstationarity in observed time-series data. Phys. Rev. E. **56**, 316–321 (1997)

Koronovskii, A.A., Hramov, A.E.: Continuous Wavelet Analysis in Application to Nonlinear Dynamics Problems. College, Saratov (2003)

Koronovskii, N.V., Abramov, V.A.: Earthquakes: causes, consequences, forecast. Soros Educ. J. **12**, 71–78, (in Russian) (1998)

Kugiumtzis, D., Lingjaerde, O.C., Christophersen, N.: Regularized local linear prediction of chaotic time series. Phys. D. **112**, 344–360 (1998)

Lachaux, J.P., Rodriguez, E., Le Van Quyen, M., et al.: Studying single-trials of phase synchronous activity in the brain. Int. J. Bif. Chaos. **10**, 2429–2455 (2000)

Lean, J., Rottman, G., Harder, J., Kopp, G.: Source contributions to new understanding of global change and solar variability. Solar Phys. **230**, 27–53 (2005)

Lequarre, J.Y.: Foreign currency dealing: a brief introduction (data set C). In: Gerschenfeld, N.A., Weigend, A.S. (eds.) Time Series Prediction: Forecasting the Future and Understanding the Past. SFI Studies in the Science of Complexity, Proc. V. XV, pp. 131–137. Addison-Wesley, New York (1993)

Letellier, C., Le Sceller, L., Gouesbet, G., et al.: Recovering deterministic behavior from experimental time series in mixing reactor. AIChE J. **43**(9), 2194–2202 (1997)

Letellier, C., Macquet, J., Le Sceller, L., et al. On the non-equivalence of observables in phase space reconstructions from recorded time series. J. Phys. A: Math. Gen. **31**, 7913–7927 (1998)

Ljung, L.: System Identification. Theory for the User. Prentice-Hall, New York (1991)

Makarenko, N.G.: Embedology and neuro-prediction. Procs. V All-Russian Conf. "Neuroinformatics-2003". Part 1, pp. 86–148, Moscow, (in Russian) (2003)

Maraun, D., Kurths, J.: Cross wavelet analysis: significance testing and pitfalls. Nonlin. Proc. Geophys. **11**, 505–514 (2004)

Marwan, N., Kurths, J.: Nonlinear analysis of bivariate data with cross recurrence plots. Phys. Lett. A. **302**, 299–307 (2002)

Marwan, N., Kurths, J.: Cross recurrence plots and their applications. In: Benton, C.V. (ed.) Mathematical Physics Research at the Cutting Edge, pp. 101–139. Nova Science Publishers, Hauppauge (2004)

Marwan, N., Romano, M.C., Thiel, M., Kurths, J.: Recurrence plots for the analysis of complex systems. Phys. Rep. **438**, 237–329 (2007)

Marwan, N.: Encounters with Neighbours – Current Developments of Concepts Based on Recurrence Plots and Their Applications. Ph.D. Thesis. University of Potsdam, Potsdam (2003)

Misiti, R. et al. Wavelet Toolbox. User Guide for MatLab. The second edition (2000)

Monin, A.S., Piterbarg, L.I.: About predictability of weather and climate. In: Kravtsov, Yu.A. (ed.) Limits of Predictability, pp. 12–39. TsentrCom, Moscow, (in Russian) (1997)

Mudrov, V.L., Kushko, V.L.: Methods of Measurement Processing. Sov. Radio, Moscow, (in Russian) (1976)

Pecora, L.M., Carroll, T.L., Heagy, J.F.: Statistics for mathematical properties of maps between time series embeddings. Phys. Rev. E. **52**, 3420–3439 (1995)

Pikovsky, A.S., Rosenblum, M.G., Kurths, J.: Synchronisation. A Universal Concept in Nonlinear Sciences. Cambridge University Press, Cambridge (2001)

Press, W.H., Flannery, B.P., Teukolsky, S.A., Vetterling, W.T.: Numerical Recipes in C. Cambridge University Press, Cambridge (1988)

Priestley, M.B.: Spectral Analysis and Time Series. Academic, London (1989)

Pugachev, V.S.: Theory of Probabilities and Mathematical Statistics. Nauka, Moscow, (in Russian) (1979)

Pugachev, V.S.: Probability Theory and Mathematical Statistics for Engineers. Pergamon Press, Oxford (1984)

Rabiner, L.R., Gold, B.: Theory and Applications of Digital Signal Processing. Prentice Hall, New York (1975)

Rieke, C., Sternickel, K., Andrzejak, R.G., Elger, C.E., David, P., Lehnertz, K.: Measuring nonstationarity by analyzing the loss of recurrence in dynamical systems. Phys. Rev. Lett. **88**, 244102 (2002)

Rigney, D.R., Goldberger, A.L., Ocasio, W.C., et al.: Multi-channel physiological data: Description and analysis (data set B). In: Gerschenfeld, N.A., Weigend, A.S. (eds.) Time Series Prediction: Forecasting the Future and Understanding the Past. SFI Studies in the Science of Complexity, Proc. V. XV, pp. 105–129. Addison-Wesley, New York (1993)

Rulkov, N.F., Sushchik, M.M., Tsimring, L.S., Abarbanel, H.D.I.: Generalized synchronization of chaos in directionally coupled chaotic systems. Phys. Rev. E. **51**, 980–994 (1995)

Sadovsky, M.A., Pisarenko, V.F.: About time series forecast. In: Kravtsov, Yu.A. (ed.) Limits of Predictability, pp. 158–169. TsentrCom, Moscow (in Russian) (1997)

Sato, M., Hansen, J.E., McCormick, M.P., Pollack, J.B.: Stratospheric aerosol optical depths, 1850–1990. J. Geophys. Res. **98**, 22987–22994 (1993)

Schiff, S.J., So, P., Chang, T., Burke, R.E., Sauer, T.: Detecting dynamical interdependence and generalized synchrony through mutual prediction in a neural ensemble. Phys. Rev. E. **54**, 6708–6724 (1996)

Schreiber, T.: Detecting and analyzing nonstationarity in a time series using nonlinear cross predictions. Phys. Rev. Lett. **78**, 843–846 (1997)

Schreiber, T.: Interdisciplinary application of nonlinear time series methods. Phys. Rep. **308**, 3082–3145 (1999)

Sena, L.A.: Units of Physical Quantities and Their Dimensions. Nauka, Moscow (1977). Translated into English: Mir Publ., Moscow (1982)

Soofi, A.S., Cao, L. (eds.): Modeling and Forecasting Financial Data: Techniques of Nonlinear Dynamics. Kluwer, Dordrecht (2002)

Timmer, J., Lauk, M., Pfleger, W., Deuschl, G.: Cross-spectral analysis of physiological tremor and muscle activity. I. Theory and application to unsynchronized elecromyogram. Biol. Cybern. **78**, 349–357 (1998)

Torrence, C., Compo, G. A prectical guide to wavelet analysis. Bull. Amer. Meteor. Soc. **79**, 61–78 (1998)

Trubetskov, D.I.: Oscillations and Waves for Humanitarians. College, Saratov, (in Russian) (1997)

von Mises, R.: Mathematical Theory of Probability and Statistics. Academic Press, New York (1964)

Yule, G.U.: On a method of investigating periodicities in disturbed series, with special reference to Wolfer's sunspot numbers. Phil. Trans. R. Soc. London A. **226**, 267–298 (1927)

Zbilut, J.P., Giuliani, A., Webber, C.L.: Detecting deterministic signals in exceptionally noisy environments using cross-recurrence quantification. Phys. Lett. A. **246**, 122–128 (1998)